

# Robust Secure UAV Relay-Assisted Cognitive Communications with Resource Allocation and Cooperative Jamming

Zhen Wang, Jichang Guo, Zhiqiong Chen, Lisu Yu, Yuhao Wang, and Hong Rao

**Abstract**—This paper considers a novel scenario, where a physical layer security issue is studied in unmanned aerial vehicles (UAVs)-assisted cognitive relay system. A secondary unmanned aerial vehicle (SUAV) relay delivers information from multiple secondary Internet of things (IoT) devices to a secondary user (SU) under the spectrum sharing with primary users (PUs). In the processing of the information transmission of the SUAV relay, a secondary eavesdropper (SE) wiretaps the information transmitted by the UAV relay with imperfect location information. In order to confuse the SE, a friendly SUAV jammer is employed to transmit jamming signals to the SE. To prevent the SE wiretapping information as much as possible, we aim to maximize average worst-case secrecy rate of the secondary relay network by jointly optimizing robust trajectories and power of the SUAV relay and jammer under the power, trajectories, information causality and multiple interference temperature (IT) threshold constraints. Thus, we formulate the original problem which is a challenging non-convex problem. We propose an effective algorithm to solve the original problem and attain locally optimal solution based on the successive convex approximation (SCA) technology and the alternate optimization method. Simulations are offered to demonstrate that our proposed resource allocation scheme can effectively improve the security performance of the SUAV relay network in comparison with other benchmark schemes.

**Index Terms**—Physical layer security, resource allocation, robust trajectory, UAV cognitive relay, UAV jammer.

## I. INTRODUCTION

**D**UE to the advantages of rapid deployment, low-altitude flight, line-of-sight (LoS) communication link and wide

This work was supported in part by the National Science Foundation of China (NSFC) under Grant 62161024, 62061030 and 81960325, China Postdoctoral Science Foundation under Grant 2021TQ0136, the State Key Laboratory of Computer Architecture (ICT, CAS) Open Project under Grant CARCB202019, and the Key Research and Development Project of Jiangxi Province under Grant 20202BBE53019.

Manuscript received August 31, 2021; revised November 26, 2021; approved for publication by Hongliang Zhang, Guest Editor, December 7, 2021.

Z. Wang is with School of Artificial Intelligence, Beijing University of Posts and Telecommunications, Beijing 100876, China, and also with School of Information Engineering, Nanchang University, Nanchang 330031, China, email: wangzhen@ncu.edu.cn.

J. Guo, Z. Chen, L. Yu, and H. Rao are with School of Information Engineering, Nanchang University, Nanchang 330031, China, email: guojichang@email.ncu.edu.cn; zhiqiongchenncu@163.com; lisuyu@ncu.edu.cn; raohong@ncu.edu.cn.

Y. Wang is with Artificial Intelligence Industry Institute, Nanchang University, Nanchang 330031, China, and also with Shangrao Normal University, Shangrao 334001, China, email: wangyuhao@ncu.edu.cn.

L. Yu is the corresponding author.

Digital Object Identifier: 10.23919/JCN.2021.000044

coverage, unmanned aerial vehicle (UAV) plays an important role in various practical scenarios, such as post-disaster rescue, cargo transport and emergency communication [1], which have brought great commercial benefits. With the widespread application of 5G technology in recent years, the scientific and technological workers pay more and more attention to the field of wireless communication [2]. Unmanned aerial vehicles (UAVs) are widely used in wireless communication network with their many characteristics. For example, when a UAV communicates with multiple ground nodes, the UAV performs data collection [3]–[6], information transmission as a relay [7] and data edge computing [8], [9]. Therefore, in the wireless communication network, the application of UAV can not only improve the speed and quality of communication, but also effectively reduce the cost of communication facilities.

### A. Related Work and Motivation

For the research and application of UAV in wireless communication network, we have investigated the relevant work in recent years. When there is long distance or towering obstacles between the signal transmitter and the signal receiver, the communication will be hindered and the communication quality will be seriously reduced. In these scenarios, we can let the UAV act as a relay to provide information transmission services, which can not only improve the communication quality, but also expand the communication distance. It is worth noting that there are two types of UAV relay, one type is static relay [10]–[13] and the other is dynamic relay [14]–[18]. The research aim of the static relay is to find the best hover point in the wireless communication network, so as to enhance the overall system performance. The authors of [10] maximized the system reliability by using a static UAV as a relay. In [11], by optimizing the static location of UAV, the authors successfully maximized the throughput of the UAV relay assisted wireless communication system. In addition, the authors of [12] constructed a channel model and a relay protocol to effectively maximize the signal-to-noise ratio (SNR) of the system by optimizing the locations of the relay UAVs. In reference [13], the position of a UAV relay was optimized with the power and SNR constraints to maximize the total communication data rate of the system.

In recent years, a UAV-enabled mobile relay has become a research hotspot, and has been widely concerned by scholars and experts [14]–[18]. In [14], the authors researched the problem of throughput maximization by constructing an UAV

Creative Commons Attribution-NonCommercial (CC BY-NC).

This is an Open Access article distributed under the terms of Creative Commons Attribution Non-Commercial License (<http://creativecommons.org/licenses/by-nc/3.0>) which permits unrestricted non-commercial use, distribution, and reproduction in any medium, provided that the original work is properly cited.

to act as a mobile relay. A rotary-wing UAV was used as a mobile relay in [15], the flight trajectory and the power distribution and the communication time of the UAV were optimized to minimize the energy consumption. The authors in [16] proposed a UAV-assisted relay network, the capacity of which was maximized. In [17], the authors considered a mobile relay network to minimize the outage probability. In addition, a UAV relay was applied to help communication in the cell edge [18]. Compared with UAV relays in fixed locations, mobile UAV relays can be more flexible to improve the quality of communication.

It is worth noting that a UAV is applied in the wireless cognitive network to improve the spectrum utilization. Thus, we make some surveys about the research of the cognitive UAV [19]–[24]. In cognitive UAV networks, the researchers proposed a spectrum sensing scheme [19], a power control algorithm [20] and a S-Procedure algorithm [21] to maximize the system throughput. By combining with the non-orthogonal multiple access (NOMA) technology [22] or the interference threshold limit [23] in the cognitive system, the system secrecy rate was maximized. In a UAV assisted cognitive system, the authors maximized the transmission rate of secondary users by optimizing the UAV's power and its path [24]. In addition to [20], the literatures [19]–[24] do not consider a UAV-assisted cognitive relay systems. Although the authors of [20] studied cognitive UAV relay in wireless communication system, they do not consider the system secrecy rate.

In the wireless communication systems, the information transmission security which is paid much attention is also research hotspot at present. Therefore, we have done a lot of investigations on secure UAVs [25]–[32]. In references [25], [26], the authors proposed an artificial noise (AN) method and the means of joint trajectory and power optimization to resist eavesdropping and improve system secrecy rate, respectively. In [27], [28], the authors maximize secrecy rate of the UAV relay with a UAV jammer and an active eavesdropper whose location is not fixed. An effective method was proposed to achieve the best security performance of the system with multiple randomly distributed eavesdroppers in [29]. The authors in [30] considered resource allocation for secure multi-UAV communication systems with multiple eavesdroppers. In [31], [32], the application of a friendly jamming UAV can maximize the system confidentiality in the presence of multiple eavesdroppers. However, the authors of [25]–[32] do not considered the system security of the UAV relay in cognitive networks.

## B. Contributions and Organization

In this paper, we study a security issue of the cognitive system based on two secondary UAVs (SUAVs), which are the secondary UAV relay (SUAV  $R$ ) and the secondary UAV jammer (SUVA  $J$ ). In addition to the SUAVs, there are multiple primary users (PUs), multiple secondary internet of things devices (SIoTs), a secondary user (SU) as well as a secondary eavesdropper (SE) in the cognitive system, where we aim to maximize secrecy rate of the secondary relay network. For our works, the main contributions are summarized as follows:

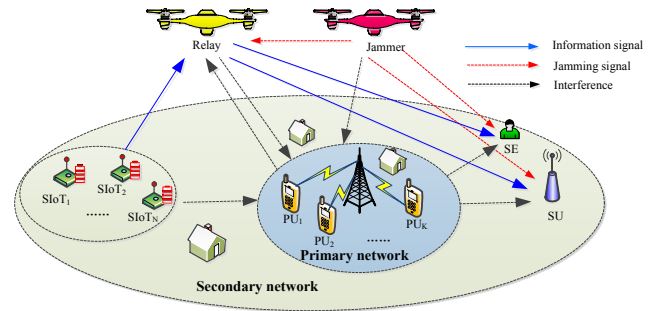


Fig. 1. The system model.

- A novel design about the physical layer security of the secondary relay network is made. In the secondary network, the mission of the SUAV  $R$  is to transmit data from the SIoTs to the SU. Around the SU, there is a SE whose accurate location is not known wiretaps the information of the SUAV  $R$ . In order to prevent the SE wiretapping information, we introduce a friendly SUAV  $J$  to disturb the SE. In order to maximize the average worst-case secrecy rate of the secondary network, we formulate a primal problem, where the transmit power of each secondary Internet of things device (SIoT) and the SUAVs should be restrained to avoid the interference for the PUs based on IT constraints.
- Since the proposed problem is a non-convex problem which is difficult to solve directly, an effective approach is proposed to solve it. Specifically, we divide the primal problem to three sub problems. Under the uncertain location of the SE, we can estimate the SE' location according to the offered range value of location estimation. By adopting alternating optimization and successive convex approximation (SCA) means, we optimize three sub problems alternately to attain the locally optimal solution of the primal problem through multiple iterations.
- Simulation results show the effectiveness of the proposed algorithm by comparing other benchmark designs. That is to say, the average worst-case secrecy rate based on our proposed algorithm is best in comparison with that based on other different designed algorithms. Our proposed algorithm is also shown to converge quickly via the convergence simulation of the algorithm results.

The rest organization of the paper is arranged as follows. In Section II, a novel secure relay system model and an optimization problem are proposed in the cognitive network. In Section III, the scheme and algorithm of convex processing for the initial problem is proposed to maximize the average secrecy rate. In Section IV, our proposed algorithm is proved to be effective and fast convergent through the analysis of simulation results. In Section V, we conclude this paper.

## II. SYSTEM MODEL AND PROBLEM FORMULATION

### A. System Model

As shown in Fig. 1, we consider UAV relay-assisted cognitive communication systems, where the users of the secondary

network and the primary network share the same spectrum resource considering interference control with each other. In the secondary network, the SIoT  $n$  and the SU are fixed at terrestrial locations  $w_n = (x_n, y_n)$ ,  $n \in \tilde{\mathcal{N}} = \{1, 2, \dots, N\}$  and  $w_s = (x_s, y_s)$  in horizontal coordinate, respectively. The positions of the  $k$ th primary user (PU) which is stationed in ground is expressed as  $w_{P,k} = (x_{P,k}, y_{P,k})$ ,  $k \in \hat{\mathcal{K}} = \{1, 2, \dots, K\}$ , where  $K$  represents the total number of the PUs in the primary network. The SIOts cannot communicate directly with the SU on account of the transmission signals attenuation of long distance communication and the interference of the subsistent PUs between the SIOts and the SU. So we deploy a SUAV  $R$  to delivery effectively information from the SIOts to the SU in the secondary network under a tolerable level of the caused interference for the PUs. However, a ground SE conceals near the SU to steal the information of the SUAV  $R$ . Although the exact location of the SE is not known, its approximate location is known by SUAVs with maximum range estimation value  $\pi$ . Let  $\hat{w}_e$  and  $w_e$  denote the estimated location and the exact location of the SE, respectively. According to the location error model [33], there is  $w_e \in \Omega = \{\|\hat{w}_e - w_e\| \leq \pi\}$ , where  $\|\cdot\|$  represents the Euclidean norm. So we add a SUAV  $J$  to disturb information interception of the SE in order to enhance the information secrecy rate of the secondary network.

We consider that the SUAVs accomplish mission with total flight time  $T$ , which is discretized into  $L - 1$  time slots with equal duration  $\delta_s = T/(L - 1)$ . Similarly, the trajectory of SUAVs is discretized as  $L$  discrete locations by optimizing to divide the trajectory into  $L - 1$  line segments. Let  $\mathcal{L} = \{1, 2, \dots, L\}$  denote a set of time slots. The SUAV  $m$ ,  $m \in \{R, J\}$ , includes the SUAV  $R$  and SUAV  $J$  based on  $m$ . At any time slot  $l$ ,  $l \in \mathcal{L} = \{1, 2, \dots, L\}$ ,  $\mathbf{q}_m[l] = (x_m[l], y_m[l]) \in \mathbb{R}^{2 \times 1}$  denotes the horizontal locations of the SUAV  $m$ ,  $m \in \{R, J\}$  in this paper, where  $\mathbb{R}^{2 \times 1}$  is on behalf of the space of 2-dimensional real vector and the boldface letter represents vector. Each SUAV  $m$  with constant altitude  $H_m$  flies from the set initial location  $\mathbf{q}_m[1]$  to the final location  $\mathbf{q}_m[L]$  at maximum displacement  $\hat{V}_{\max} = V_{\max} \delta_s$  limit between two successive time slots, i.e.,  $\|\mathbf{q}_m[l+1] - \mathbf{q}_m[l]\| \leq \hat{V}_{\max}$ ,  $l \in \hat{\mathcal{L}} = \{1, 2, \dots, L-1\}$ , where  $V_{\max}$  denotes maximum flight speed of the SUAV  $m$ ,  $m \in \{R, J\}$ .

In the system model, we assume that the communication channel is dominated by LoS link [30] between the SUAV  $m$  and the SU or the SE. Due to the adopted free-space path loss model [30], the power gain of wireless channel between the SUAV  $R$  and the SIoT  $n$  at time slot  $l \in \mathcal{L}$  is attained as

$$h_{n,R}[l] = \frac{\beta_0}{d_{n,R}^2[l]} = \frac{\beta_0}{\|\mathbf{q}_R[l] - w_n\|^2 + H_R^2}, n \in \tilde{\mathcal{N}}, \quad (1)$$

where  $\beta_0$  represents the power gain of channel at reference unit distance of 1 meter, and  $d_{n,R}[l] = \sqrt{\|\mathbf{q}_R[l] - w_n\|^2 + H_R^2}$  denotes the straight line distance between the SUAV  $R$  and the SIoT  $n$ . Similarly, the power gain of wireless channel during the information transmission from the SUAV  $m$  to the SU at

any slot  $l$ ,  $\forall l \in \mathcal{L}$ , is written as

$$h_{m,S}[l] = \frac{\beta_0}{d_{m,S}^2[l]} = \frac{\beta_0}{\|\mathbf{q}_m[l] - w_s\|^2 + H_m^2}, m \in \{R, J\}, \quad (2)$$

where  $d_{m,S}[l] = \sqrt{\|\mathbf{q}_m[l] - w_s\|^2 + H_m^2}$  denotes the straight line distance of data transfer from the SUAV  $m$  to the SU. Based on the distance  $d_{m,E}[l] = \sqrt{\|\mathbf{q}_m[l] - w_e\|^2 + H_m^2}$  from the SUAV  $m$  to the SE, the power gain of wireless channel between the SUAV  $m$  and the SE at any slot  $l$ ,  $\forall l \in \mathcal{L}$ , is written similarly as

$$h_{m,E}[l] = \frac{\beta_0}{d_{m,E}^2[l]} = \frac{\beta_0}{\|\mathbf{q}_m[l] - w_e\|^2 + H_m^2}, m \in \{R, J\}. \quad (3)$$

In UAV-to-ground and UAV-to-UAV channels, we suppose that the Doppler effect generated by mobility of UAVs is ideally offset [34]. Thus, the power gain of the channel between the SUAV  $R$  and the SUAV  $J$  by adopting the free-space path loss model [30] at any slot  $l$ ,  $\forall l \in \mathcal{L}$ , is attained as

$$h_{J,R}[l] = \frac{\beta_0}{d_{J,R}^2[l]} = \frac{\beta_0}{\|\mathbf{q}_R[l] - \mathbf{q}_J[l]\|^2 + (H_R - H_J)^2}, \quad (4)$$

where  $d_{J,R}[l] = \sqrt{\|\mathbf{q}_R[l] - \mathbf{q}_J[l]\|^2 + (H_R - H_J)^2}$  denotes the straight-line distance between the SUAV  $R$  and the SUAV  $J$ . In the secondary network, we assume that the data transmission mechanism of SUAV  $R$  with the adequate data caches from the SIOts to the SU is adopted the frequency division dual (FDD) mechanism of the full-duplex mode [35]. At time slot  $l$ , suppose that each SIoT transmits information to the SUAV  $R$  simultaneously by adopting the frequency division multiple access (FDMA) mechanism [36]. Although the frequency bands of information transmission of each SIoT and the SUAV  $R$  are different in the secondary network, these frequency bands of the secondary network are all within the spectrum range of the cognitive wireless network and are shared with the PUs of the primary network [36]. The interferences of the SUAV  $R$  and the SU come from the amicable SUAV  $J$  and the PUs. The transmission signal of the SUAV  $J$  is deemed as noise for the SUAV  $R$ , the SU and the SE [37]. We assume that the interference of the SUAV  $R$ , the SU and the SE from the PUs is circularly symmetric complex Gaussian which is the worst case interference model [38]. The interference model has been widely used in [38]. Thus, the signal transmission rate from the SIoT  $n$  to the SUAV  $R$  at slot  $\forall l \in \mathcal{L}$  in bit/second/Hertz (bps/Hz) is written as

$$R_{n,R}[l] = \log_2 \left( 1 + \frac{h_{n,R}[l]P_n[l]}{h_{J,R}[l]P_J[l] + \delta_a^2} \right), n \in \tilde{\mathcal{N}}, \quad (5)$$

where  $P_n[l]$  and  $P_J[l]$  represent transmission power of the SIoT  $n$  and the SUAV  $J$ , respectively.  $\delta_a^2$  is on behalf of the total power of receiver noise and the primary network interference at the SUAV  $R$  and the SU [24], [38]. And  $h_{J,R}[l]P_J[l]$  denotes the jamming power caused by the SUAV  $J$  [33]. Analogously, via the information delivery of the SUAV  $R$  from ground the SIoT  $n$  to the SU, the reception rate of

the information transmitted by the SUAV  $R$  for the SU is expressed as

$$R_{R,S}[l] = \log_2 \left( 1 + \frac{h_{R,S}[l]P_R[l]}{h_{J,S}[l]P_J[l] + \delta_a^2} \right), \forall l, \quad (6)$$

where  $P_R[l]$  represents transmission power of the SUAV  $R$ . Similarly, the rate of data wiretap for the SE is written as

$$R_{R,E}[l] = \log_2 \left( 1 + \frac{h_{R,E}[l]P_R[l]}{h_{J,E}[l]P_J[l] + \delta_a^2} \right), \forall l. \quad (7)$$

In the relay network, the information transmission of SUAV  $R$  should comply with information causality, i.e., the total information bits received by the SU cannot exceed the total bits of information sent by all SIOs over  $l$  time slots,  $l \in \mathcal{L}$ . On account of the information dispose demand of one time slot in the process of the SUAV  $R$  forwarding information, the SU do not receive information in the first time slot and the SIO  $n$  do not send information in the last time slot, i.e.,  $R_{R,S}[1] = 0$  and  $R_{n,R}[N] = 0$ . Thus, the information causality of the secondary relay network is expressed as

$$\sum_{r=2}^l R_{R,S}[r] \leq \sum_{r=1}^{l-1} \sum_{n=1}^N R_{n,R}[r], l \in \tilde{\mathcal{L}} = \{2, \dots, L\}. \quad (8)$$

However, the transmit power of each SIO  $n$  and the SUAV  $m$ ,  $m \in \{R, J\}$  in the secondary network will generate interference to the all PUs' communication of the primary network. So the interference temperature (IT) method [39] is adopted to safeguard the communication quality of all PUs. We define  $\Gamma^S$  and  $\Gamma^{RJ}$  as the tolerant IT thresholds of every PU  $k$  for the SIO  $n$ , for the SUAV  $R$  and the SUAV  $J$ , respectively. Within the tolerant IT thresholds  $\Gamma^S$  and  $\Gamma^{RJ}$ , the communication quality of all PUs will not be affected. Considered that the SIO  $n$  and PU  $k$  are fixed on the surface of land, the channel model between the SIO  $n$  and the PU  $k$  is supposed to abide by the independent Rayleigh fading model with the channel power gain  $h_{n,k} = \beta_0 d_{n,k}^{-\lambda} \xi$ , where  $\lambda$  and  $\xi$  denote the path loss exponent and an exponentially distributed random variable with mean one, respectively [23], [40]. And  $d_{n,k}$  represents the distance between the SIO  $n$  and the PU  $k$ ,  $n \in \tilde{\mathcal{N}}$ ,  $k \in \hat{\mathcal{K}}$ . According to Rayleigh fading model, the IT constrain of each SIO based on average interference in order to protect the PU  $k$  is written as

$$\mathbb{E}_\xi \left[ \frac{\beta_0 P_n[l]}{(\|\mathbf{w}_n - \mathbf{w}_{P,k}\|)^\lambda} \xi \right] \leq \Gamma^S, n \in \tilde{\mathcal{N}}, k \in \hat{\mathcal{K}}, \quad (9)$$

where  $\mathbb{E}_\xi[\cdot]$  denotes the mathematical expectation with random variable  $\xi$ . Since the channel model between the SIO  $n$  and the PU  $k$  is supposed to follow the independent Rayleigh fading model [23], [40], we can deal with the left item of formula (9) to acquire  $\mathbb{E}_\xi \left[ \frac{\beta_0 P_n[l]}{(\|\mathbf{w}_n - \mathbf{w}_{P,k}\|)^\lambda} \xi \right] = \frac{\beta_0 P_n[l]}{(\|\mathbf{w}_n - \mathbf{w}_{P,k}\|)^\lambda} \mathbb{E}_\xi[\xi]$ , where  $\mathbb{E}_\xi[\xi]$  is a constant term with value one. Thus, we can also acquire  $\mathbb{E}_\xi \left[ \frac{\beta_0 P_n[l]}{(\|\mathbf{w}_n - \mathbf{w}_{P,k}\|)^\lambda} \xi \right] = \frac{\beta_0 P_n[l]}{(\|\mathbf{w}_n - \mathbf{w}_{P,k}\|)^\lambda}$ . Therefore, the formula (9) can be rewritten as

$$\frac{\beta_0 P_n[l]}{(\|\mathbf{w}_n - \mathbf{w}_{P,k}\|)^\lambda} \leq \Gamma^S, n \in \tilde{\mathcal{N}}, k \in \hat{\mathcal{K}}. \quad (10)$$

Due to the SUAV  $R$  and SUAV  $J$  in the air, the channel between the SUAV  $m$ ,  $m \in \{R, J\}$  and all ground PUs is considered as the LoS channel. Based on the LoS channel model, the IT constrains which can protect all PUs from the interference of the SUAV  $R$  and SUAV  $J$  at any slot  $l$  are respectively given by

$$\frac{\beta_0 P_R[l]}{\|\mathbf{q}_R[l] - \mathbf{w}_{P,k}\|^2 + H_R^2} \leq \Gamma^{RJ}, k \in \hat{\mathcal{K}}, \quad (11)$$

$$\frac{\beta_0 P_J[l]}{\|\mathbf{q}_J[l] - \mathbf{w}_{P,k}\|^2 + H_J^2} \leq \Gamma^{RJ}, k \in \hat{\mathcal{K}}. \quad (12)$$

## B. Problem Formulation

Since the exact location of the SE can't be fully known by SUAV  $m$ ,  $m \in \{R, J\}$ , we more concern about the worst-case secrecy rate of the secondary relay network. Thus, the worst-case secrecy rate from the SUAV  $R$  to the SU in bps/Hz at  $l$  time slots is expressed as

$$R_{ser}[l] = \left[ R_{R,S}[l] - \max_{\mathbf{w}_e \in \Omega} R_{R,E}[l] \right]^+, \forall l, \quad (13)$$

where  $[x]^+ = \max(x, 0)$ . In the cognitive system, our goal is to maximize the average secrecy rate of the information transmission of the SUAV  $R$  by jointly optimizing the trajectories and transmit power of the SUAV  $R$  and the SUAV  $J$  based on the information causality constrain. We define  $\mathcal{P} \triangleq \{P_n[l], P_R[l], P_J[l]\}$  and  $\mathcal{Q} \triangleq \{\mathbf{q}_R[l], \mathbf{q}_J[l]\}$  in order to simplify notation expression. The optimization problem is formulated as

$$(P1) : \max_{\mathcal{P}, \mathcal{Q}} \frac{1}{L} \sum_{l=1}^L R_{ser}[l] \quad (14a)$$

$$\text{s.t. } \frac{1}{L} \sum_{l=1}^L P_n[l] \leq \bar{P}_T, 0 \leq P_n[l] \leq P_T^{\max}, n \in \tilde{\mathcal{N}}, \quad (14b)$$

$$\frac{1}{L} \sum_{l=1}^L P_R[l] \leq \bar{P}_R, 0 \leq P_R[l] \leq P_R^{\max}, \quad (14c)$$

$$\frac{1}{L} \sum_{l=1}^L P_J[l] \leq \bar{P}_J, 0 \leq P_J[l] \leq P_J^{\max}, \quad (14d)$$

$$\|\mathbf{q}_m[l+1] - \mathbf{q}_m[l]\| \leq \hat{V}_{\max}, l \in \hat{\mathcal{L}}, m \in \{R, J\} \quad (14e)$$

$$\mathbf{q}_R[1] = \mathbf{q}_R^{ini}, \mathbf{q}_R[L] = \mathbf{q}_R^{fin}, \quad (14f)$$

$$\mathbf{q}_J[1] = \mathbf{q}_J^{ini}, \mathbf{q}_J[L] = \mathbf{q}_J^{fin}, \quad (14g)$$

$$\|\mathbf{q}_R[l] - \mathbf{q}_J[l]\|^2 + (H_R - H_J)^2 \geq d_{\min}^2, \quad (14h)$$

$$(8), (10), (11), \text{ and } (12), \quad (14i)$$

where the constraints (14b), (14c), and (14d) are on behalf of the average power limitation and the peak power limitation of the SIO  $n$ , the SUAV  $R$  and the SUAV  $J$ , respectively. The  $\bar{P}_T$ ,  $\bar{P}_R$  and  $\bar{P}_J$  represent the average power of the SIO  $n$ , the SUAV  $R$  and the SUAV  $J$ , respectively. In (14b)–(14d), the transmit power of the SIO  $n$ , the SUAV  $R$  and the SUAV  $J$  at any time slot  $l$  cannot exceed the set peak power  $P_T^{\max}$ ,  $P_R^{\max}$  and  $P_J^{\max}$ , respectively. In (14f),  $\mathbf{q}_R^{ini}$  and  $\mathbf{q}_R^{fin}$  denote the initial point and final point of the SUAV  $R$ , respectively. The

constraint (14g) indicates that the SUAV  $J$  flies from the set initial location  $\mathbf{q}_J^{ini}$  to the set final location  $\mathbf{q}_J^{fin}$ . In (14h), the distance between the SUAV  $R$  and the SUAV  $J$  is greater than the minimum safe distance  $d_{min}$  in order to prevent colliding each other.

In problem (P1), we note that the objective function (14a) which includes a operator  $[\cdot]^+$  and a “max” operation is a non-concave function. Due to the coupling correlation of multiple optimization variables, the constraints (8), (11), and (12) are all non-convex. Therefore, the problem (P1) is a non-convex problem. In Section III, we will tackle the objective function and the non-convex constraint conditions in order to transform the non-convex problem (P1) into the convex problem. And we will obtain the locally optimal solution of the problem (P1) by putting forward an effective optimization algorithm.

### III. PROPOSED SOLUTION TO PROBLEM

In this section, we first tackle the uncertain expression  $\max_{\mathbf{w}_e \in \Omega} R_{R,E}[l]$  to an explicit expression. Due to the location uncertainty of the SE, the SUAV  $R$  and the SUAV  $J$  only attain it's the estimated location in the estimation range. According to the expression of the formula (7), we have

$$\max_{\mathbf{w}_e \in \Omega} R_{R,E}[l] = \log_2 \left( 1 + \frac{\max_{\mathbf{w}_e \in \Omega} h_{R,E}[l] P_R[l]}{\min_{\mathbf{w}_e \in \Omega} h_{J,E}[l] P_J[l] + \delta_a^2} \right). \quad (15)$$

On the basis of the simple derivation and proof of the literatures [33], [41], the optimal channel power gain  $\hat{h}_{R,E}[l]$  from the SUAV  $R$  to the SE is obtained at  $\mathbf{w}_e[l] = \hat{\mathbf{w}}_e + \frac{\mathbf{q}_R[l] - \hat{\mathbf{w}}_e}{\|\mathbf{q}_R[l] - \hat{\mathbf{w}}_e\|} \pi$ . The  $\hat{h}_{R,E}[l] \triangleq \max_{\mathbf{w}_e \in \Omega} h_{R,E}[l]$  is written as

$$\hat{h}_{R,E}[l] = \frac{\beta_0}{(\|\mathbf{q}_R[l] - \hat{\mathbf{w}}_e\| - \pi)^2 + H_R^2}. \quad (16)$$

Likewise, the power gain  $\hat{h}_{J,E}[l]$  of the worst channel from the SUAV  $J$  to the SE is acquired at  $\mathbf{w}_e[l] = \hat{\mathbf{w}}_e - \frac{\mathbf{q}_J[l] - \hat{\mathbf{w}}_e}{\|\mathbf{q}_J[l] - \hat{\mathbf{w}}_e\|} \pi$  [33], [41]. The  $\hat{h}_{J,E}[l] \triangleq \min_{\mathbf{w}_e \in \Omega} h_{J,E}[l]$  is expressed as

$$\hat{h}_{J,E}[l] = \frac{\beta_0}{(\|\mathbf{q}_J[l] - \hat{\mathbf{w}}_e\| + \pi)^2 + H_J^2}. \quad (17)$$

According to the formulas (15), (16), and (17), the upper bound rate  $\hat{R}_{R,E}[l]$  of the achievable rate between the SUAV  $R$  and the SE is written as

$$\hat{R}_{R,E}[l] = \log_2 \left( 1 + \frac{\hat{h}_{R,E}[l] P_R[l]}{\hat{h}_{J,E}[l] P_J[l] + \delta_a^2} \right). \quad (18)$$

Therefore, we can infer that  $\hat{R}_{R,E}[l]$  is the upper bound of  $\max_{\mathbf{w}_e \in \Omega} R_{R,E}[l]$ , i.e.,  $\max_{\mathbf{w}_e \in \Omega} R_{R,E}[l] \leq \hat{R}_{R,E}[l]$ . In (13), we use  $\hat{R}_{R,E}[l]$  instead of  $\max_{\mathbf{w}_e \in \Omega} R_{R,E}[l]$  to obtain the lower bound of secrecy rate, which is  $\hat{R}_{ser}[l] = \left[ R_{R,S}[l] - \hat{R}_{R,E}[l] \right]^+$  at any  $l$  time slot. Thus, we replace  $\sum_{l=1}^L R_{ser}[l]$  of the objective function (14a) with explicit function  $\sum_{l=1}^L \hat{R}_{ser}[l]$  to maximize the lower

bound value of the cumulative secrecy rate in problem (P1). Since the transmit power optimization can always make the cumulative secrecy rate non-negative [33], the  $[\cdot]^+$  is omitted in the objective function. Therefore, we approximate problem (P1) to obtain problem (P2), which is as follow

$$(P2) : \max_{\mathbf{P}, \mathbf{Q}} \frac{1}{L} \sum_{l=1}^L \left( R_{R,S}[l] - \hat{R}_{R,E}[l] \right) \quad (19a)$$

$$\text{s.t. (14b), (14c), (14d), (14e), (14f), (14g),} \quad (19b)$$

$$(8), (10), (11), \text{ and } (12). \quad (19c)$$

Nevertheless, the objective function of problem (P2) still is a non-concave function in addition to the non-convex constrains (8), (11) and (12). Thus, the problem (P2) is a non-convex problem and need to be disposed. The alternating optimization means is adopted to handle the non-convex problem (P2) in this paper. We will divide problem (P2) into three subproblems, which are the subproblem of only optimizing the trajectory  $\mathbf{q}_R[l]$  of the SUAV  $R$ , the subproblem of only optimizing the trajectory  $\mathbf{q}_J[l]$  of the SUAV  $J$ , and the subproblem of jointly optimizing the transmit power  $P_n[l]$ ,  $P_R[l]$  and  $P_J[l]$ , respectively.

#### A. Transmit Power Allocation

In this subproblem, we jointly optimizing the transmit power  $P_n[l]$  of the SiOT  $n$ , the transmit power  $P_R[l]$  of the SUAV  $R$  and the transmit power  $P_J[l]$  of the SUAV  $J$  under the given trajectories of the SUAV  $R$  and the SUAV  $J$ . Thus, the subproblem (P3) is formulated as follow

$$(P3) : \max_{\mathbf{P}} \frac{1}{L} \sum_{l=1}^L \left( R_{R,S}[l] - \hat{R}_{R,E}[l] \right) \quad (20a)$$

$$\text{s.t. (14b), (14c), (14d),} \quad (20b)$$

$$(8), (10), (11), \text{ and } (12). \quad (20c)$$

Due to the non-concave objective function in (P3), we first need to transform it to a concave function. The expansion form of the formula  $R_{R,S}[l] - \hat{R}_{R,E}[l]$  is written as

$$\begin{aligned} R_{R,S}[l] - \hat{R}_{R,E}[l] &= \log_2 \left( h_{J,S}[l] P_J[l] + \delta_a^2 + h_{R,S}[l] P_R[l] \right) \\ &+ \log_2 \left( \hat{h}_{J,E}[l] P_J[l] + \delta_a^2 \right) - \log_2 \left( h_{J,S}[l] P_J[l] + \delta_a^2 \right) \\ &- \log_2 \left( \hat{h}_{J,E}[l] P_J[l] + \delta_a^2 + \hat{h}_{R,E}[l] P_R[l] \right), \end{aligned} \quad (21)$$

where the  $\log_2 \left( h_{J,S}[l] P_J[l] + \delta_a^2 + h_{R,S}[l] P_R[l] \right)$  and  $\log_2 \left( \hat{h}_{J,E}[l] P_J[l] + \delta_a^2 \right)$  are concave terms in regard to the variables  $P_J[l]$  or  $P_R[l]$ . However, the  $-\log_2 \left( h_{J,S}[l] P_J[l] + \delta_a^2 \right)$  and  $-\log_2 \left( \hat{h}_{J,E}[l] P_J[l] + \delta_a^2 + \hat{h}_{R,E}[l] P_R[l] \right)$  are convex terms in regard to the variables  $P_J[l]$  or  $P_R[l]$  and need to be handled. The first order Taylor expansion method is applied to tackle the term  $-\log_2 \left( h_{J,S}[l] P_J[l] + \delta_a^2 \right)$  and get its lower bound function with the variable  $P_J[l]$  as follows

$$-\log_2 \left( h_{J,S}[l] P_J[l] + \delta_a^2 \right) \geq$$

$$-\log_2 \left( h_{J,S}[l]P_J^{(i)}[l] + \delta_a^2 \right) - \frac{h_{J,S}[l] \left( P_J[l] - P_J^{(i)}[l] \right)}{\ln 2 \left( h_{J,S}[l]P_J^{(i)}[l] + \delta_a^2 \right)}, \quad (22)$$

where  $P_J^{(i)}[l]$  represents the SUAV  $J$  power value of the  $i$ th iteration. For the dispose of term  $-\log_2 \left( \hat{h}_{J,E}[l]P_J[l] + \delta_a^2 + \hat{h}_{R,E}[l]P_R[l] \right)$ , we introduce the nonnegative relaxation variable  $A[l]$ . Let  $\frac{1}{A[l]} = \hat{h}_{J,E}[l]P_J[l] + \delta_a^2 + \hat{h}_{R,E}[l]P_R[l]$ . And the term  $-\log_2 \left( \hat{h}_{J,E}[l]P_J[l] + \delta_a^2 + \hat{h}_{R,E}[l]P_R[l] \right)$  is equivalent to  $\log_2(A[l])$  which is a concave function. Therefore, the objective function is rewritten as

$$\begin{aligned} & R_{R,S}[l] - \hat{R}_{R,E}[l] \\ & = \log_2 \left( h_{J,S}[l]P_J[l] + \delta_a^2 + h_{R,S}[l]P_R[l] \right) \\ & \quad + \log_2 \left( \hat{h}_{J,E}[l]P_J[l] + \delta_a^2 \right) - \log_2 \left( h_{J,S}[l]P_J^{(i)}[l] + \delta_a^2 \right) \\ & \quad - \frac{h_{J,S}[l] \left( P_J[l] - P_J^{(i)}[l] \right)}{\ln 2 \left( h_{J,S}[l]P_J^{(i)}[l] + \delta_a^2 \right)} + \log_2(A[l]) \\ & \triangleq \tilde{R}_{ser}[l]. \end{aligned} \quad (23)$$

Based on the concave dispose of the objective function of problem (P3), the (P3) is reformulated as

$$(P3.1) : \max_{\{P_n[l], P_R[l], P_J[l], A[l]\}} \frac{1}{L} \sum_{l=1}^L \tilde{R}_{ser}[l] \quad (24a)$$

$$\text{s.t. } \frac{1}{A[l]} \geq \hat{h}_{J,E}[l]P_J[l] + \delta_a^2 + \hat{h}_{R,E}[l]P_R[l] \quad (24b)$$

$$(14b), (14c), (14d), \quad (24c)$$

$$(8), (10), (11), \text{ and } (12). \quad (24d)$$

By adding a new constraint (24b), we can deduce that the objective function of problem (P3.1) is lower bound of that of problem (P3). Since the constraints (24b) and (8) are non-convex, the problem (P3.1) is still non-convex problem. The left hand side of (24b) is a convex term. Thus, we perform the first order Taylor expansion for the item  $\frac{1}{A[l]}$  as follows

$$\frac{1}{A[l]} \geq \frac{1}{A^{(i)}[l]} - \frac{A[l] - A^{(i)}[l]}{(A^{(i)}[l])^2} = \frac{2A^{(i)}[l] - A[l]}{(A^{(i)}[l])^2}, \quad (25)$$

where  $A^{(i)}[l]$  is the obtained value at the  $i$ th iteration. The formula (8) is rewritten as

$$\begin{aligned} & \sum_{r=2}^l \log_2 \left( h_{J,S}[r]P_J[r] + \delta_a^2 + h_{R,S}[r]P_R[r] \right) \\ & - \sum_{r=2}^l \log_2 \left( h_{J,S}[r]P_J[r] + \delta_a^2 \right) \\ & \leq \sum_{r=1}^{l-1} \sum_{n=1}^N \log_2 \left( h_{J,R}[r]P_J[r] + \delta_a^2 + h_{n,R}[r]P_n[r] \right) \\ & \quad - \sum_{r=1}^{l-1} \sum_{n=1}^N \log_2 \left( h_{J,R}[r]P_J[r] + \delta_a^2 \right), l \in \tilde{\mathcal{L}}. \end{aligned} \quad (26)$$

Due to the non-convexity of the term  $\log_2 \left( h_{J,S}[r]P_J[r] + \delta_a^2 + h_{R,S}[r]P_R[r] \right)$  in (26), we

introduce the nonnegative relaxation variable  $B[r]$ . We define  $\frac{1}{B[r]} = h_{J,S}[r]P_J[r] + \delta_a^2 + h_{R,S}[r]P_R[r]$ . The term  $\log_2 \left( h_{J,S}[r]P_J[r] + \delta_a^2 + h_{R,S}[r]P_R[r] \right)$  is equivalent to  $-\log_2(B[r])$  which is a convex function. Meanwhile, in optimization problem (P3.1), we add new constraint condition, which is

$$\frac{1}{B[r]} \geq h_{J,S}[r]P_J[r] + \delta_a^2 + h_{R,S}[r]P_R[r], l \in \tilde{\mathcal{L}}. \quad (27)$$

With the new constraint (27), we can deduce that  $-\log_2(B[r])$  is upper bound of  $\log_2 \left( h_{J,S}[r]P_J[r] + \delta_a^2 + h_{R,S}[r]P_R[r] \right)$  based on the monotonicity of the log function. For the non-concavity of the left side term of the constraint (27), we utilize the first order Taylor expansion to get the lower bound of the term  $\frac{1}{B[l]}$  as follow

$$\frac{1}{B[l]} \geq \frac{1}{B^{(i)}[l]} - \frac{B[l] - B^{(i)}[l]}{(B^{(i)}[l])^2} = \frac{2B^{(i)}[l] - B[l]}{(B^{(i)}[l])^2}, \quad (28)$$

where  $B^{(i)}[l]$  is the obtained value at the  $i$ th iteration. Since the right side term  $-\log_2 \left( h_{J,R}[r]P_J[r] + \delta_a^2 \right)$  of the constraint (26) is convex, the lower bound of the term  $-\log_2 \left( h_{J,R}[r]P_J[r] + \delta_a^2 \right)$  based on the first order Taylor expansion in regard to the variable  $P_J[r]$  is written as

$$\begin{aligned} & -\log_2 \left( h_{J,R}[r]P_J[r] + \delta_a^2 \right) \geq \\ & -\log_2 \left( h_{J,R}[r]P_J^{(i)}[r] + \delta_a^2 \right) - \frac{h_{J,R}[r] \left( P_J[r] - P_J^{(i)}[r] \right)}{\ln 2 \left( h_{J,R}[r]P_J^{(i)}[r] + \delta_a^2 \right)}. \end{aligned} \quad (29)$$

Based on the above convex processing of the constraint condition (26), it is rewritten as

$$\begin{aligned} & - \sum_{r=2}^l \log_2(B[r]) - \sum_{r=2}^l \log_2 \left( h_{J,S}[r]P_J[r] + \delta_a^2 \right) \\ & \leq \sum_{r=1}^{l-1} \sum_{n=1}^N \log_2 \left( h_{J,R}[r]P_J[r] + \delta_a^2 + h_{n,R}[r]P_n[r] \right) \\ & \quad - \sum_{r=1}^{l-1} N \log_2 \left( h_{J,R}[r]P_J^{(i)}[r] + \delta_a^2 \right) \\ & \quad - \sum_{r=1}^{l-1} \frac{N h_{J,R}[r] \left( P_J[r] - P_J^{(i)}[r] \right)}{\ln 2 \left( h_{J,R}[r]P_J^{(i)}[r] + \delta_a^2 \right)}, l \in \tilde{\mathcal{L}}. \end{aligned} \quad (30)$$

By the convex processing of the objective function, the constraint (8) as well as the new added constraints, we can acquire the convex approximate problem (P3.2) of the problem (P3). The problem (P3.2) is formulated as

$$(P3.2) : \max_{\{P_n[l], P_R[l], P_J[l], A[l], B[l]\}} \frac{1}{L} \sum_{l=1}^L \tilde{R}_{ser}[l] \quad (31a)$$

$$\text{s.t. } \frac{2A^{(i)}[l] - A[l]}{(A^{(i)}[l])^2} \geq \hat{h}_{J,E}[l]P_J[l] + \delta_a^2 + \hat{h}_{R,E}[l]P_R[l], \forall l, \quad (31b)$$

$$\frac{2B^{(i)}[l] - B[l]}{(B^{(i)}[l])^2} \geq h_{J,S}[r]P_J[l] + \delta_a^2 + h_{R,S}[r]P_R[l], \forall l, \quad (31c)$$

$$(14b), (14c), (14d), \quad (31d)$$

$$(10), (11), (12), \text{ and } (30). \quad (31e)$$

It is noticed that problem (P3.2) is a convex problem by the convex dispose of the objective function and the constraint (26). Since the interior point method is an optimization algorithm based on the penalty function [42], we adopt it to solve problem (P3.2) to acquire the optimal solution, which can also meet problem (P3.1). Thus, problem (P3.2) is equivalent to problem (P3.1) for the SUAVs' power allocation. Based on the constraint (24b) and the lower bound approximate of the formula (22), we can deduce that the optimization value of problem (P3.1) is the lower bound of that of problem (P3). Therefore, the optimal feasible solution of problem (P3.2) is also the feasible solution of problem (P3).

### B. Optimizing The UAV Jammer's Trajectory

In this subsection, we optimize the flight trajectory  $\mathbf{q}_J[l]$  of the SUAV  $J$  under the given the SUAV  $R$ 's trajectory  $\mathbf{q}_R[l]$  and transmit power  $P_R[l]$ , the SUAV  $J$ 's transmit power  $P_J[l]$  and the transmit power  $P_n[l]$  of the SIoT  $n$ . Thus, we are able to formulate the subproblem (P4), that is expressed as follows

$$(P4) : \max_{\mathbf{q}_J[l]} \frac{1}{L} \sum_{l=1}^L \left[ \log_2 \left( 1 + \frac{h_{R,S}[l]P_R[l]}{\frac{\beta_0 P_J[l]}{\|\mathbf{q}_J[l] - \mathbf{w}_s\|^2 + H_J^2} + \delta_a^2} \right) - \log_2 \left( 1 + \frac{\hat{h}_{R,E}[l]P_R[l]}{\frac{\beta_0 P_J[l]}{(\|\mathbf{q}_J[l] - \hat{w}_e\| + \pi)^2 + H_J^2} + \delta_a^2} \right) \right] \quad (32a)$$

$$\text{s.t. } \sum_{r=2}^l \log_2 \left( 1 + \frac{h_{R,S}[r]P_R[r]}{\frac{\beta_0 P_J[r]}{\|\mathbf{q}_J[r] - \mathbf{w}_s\|^2 + H_J^2} + \delta_a^2} \right) \leq \sum_{r=1}^{l-1} \sum_{n=1}^N \log_2 \left( 1 + \frac{h_{n,R}[r]P_n[r]}{\frac{\beta_0 P_J[r]}{\|\mathbf{q}_R[r] - \mathbf{q}_J[r]\|^2 + (H_R - H_J)^2} + \delta_a^2} \right), \quad (32b)$$

$$l \in \tilde{\mathcal{L}}, \quad (32b)$$

$$\|\mathbf{q}_J[l+1] - \mathbf{q}_J[l]\| \leq \hat{V}_{\max}, \quad (32c)$$

$$(14g), (14h), \text{ and } (12). \quad (32d)$$

Since the objective function (32a) is a non-concave function and the constraints (32b) and (14h) are non-convex in problem (P4), the problem (P4) is a non-convex problem. The slack variables  $\omega[l]$ ,  $\eta[l]$ ,  $\mu[r]$ , and  $\varphi[l]$  are introduced to the objective function and the constraints of problem (P4) so as to do convex processing for them. Thus, problem (P4) is rewritten as

$$(P4.1) : \max_{\{\mathbf{q}_J[l], \omega[l], \eta[l], \mu[r], \varphi[l]\}} \frac{1}{L} \sum_{l=1}^L [\omega[l] - \log_2 \left( 1 + \frac{\hat{h}_{R,E}[l]P_R[l]}{\frac{\beta_0 P_J[l]}{\eta[l]} + \delta_a^2} \right)] \quad (33a)$$

$$\text{s.t. } \sum_{r=2}^l \omega[r] \leq \sum_{r=1}^{l-1} \sum_{n=1}^N \log_2 \left( 1 + \frac{h_{n,R}[r]P_n[r]}{\frac{\beta_0 P_J[r]}{\mu[r]} + \delta_a^2} \right), l \in \tilde{\mathcal{L}}, \quad (33b)$$

$$\omega[l] \leq \log_2 \left( 1 + \frac{h_{R,S}[l]P_R[l]}{\frac{\beta_0 P_J[l]}{\varphi[l]} + \delta_a^2} \right), \quad (33c)$$

$$(\|\mathbf{q}_J[l] - \hat{w}_e\| + \pi)^2 + H_J^2 \leq \eta[l], \quad (33d)$$

$$\|\mathbf{q}_R[l] - \mathbf{q}_J[l]\|^2 + \Delta H^2 \geq \mu[l], \quad (33e)$$

$$\|\mathbf{q}_J[l] - \mathbf{w}_s\|^2 + H_J^2 \geq \varphi[l], \quad (33f)$$

$$\|\mathbf{q}_R[l] - \mathbf{q}_J[l]\|^2 + \Delta H^2 \geq d_{\min}^2, \quad (33g)$$

$$\frac{\beta_0 P_J[l]}{\Gamma^{RJ}} \leq \|\mathbf{q}_J[l] - \mathbf{w}_{P,k}\|^2 + H_J^2, \quad (33h)$$

$$(14g), \quad (33i)$$

where  $\Delta H = H_R - H_J$ , and the (33h) is the transformation form of (12) due to the positive  $\Gamma^{RJ}$  and  $\|\mathbf{q}_J[l] - \mathbf{w}_{P,k}\|^2 + H_J^2$ . In problem (P4.1), the new objective function (33a) and the added constraints (33c), (33d), and (33f) replace the objective function (32a) of problem (P4). From the inequalities (33c), (33d), and (33f), we can easily deduce that the objective function (33a) is the lower bound of (32a). By adding the constraint (33e), we can observe that the right hand side (RHS) term of (33b) is the lower bound of that of (32b). In constraint (33f), there exists always a feasible solution  $\mathbf{q}_J[l]$  to meet the inequalities (33f) equal by decreasing variable  $\varphi[l]$ . Meanwhile, the feasible solution  $\mathbf{q}_J[l]$  satisfies also the constraint (32b) of problem (P4). Thus, the constraint (33b) is equivalent to the constraint (32b) by adding new constraints (33c), (33e) and (33f). This indicates that the problem (P4.1) is an approximate problem of (P4). Although the constraints (33b), (33c), (33d) and (14g) are convex constraints in problem (P4.1), the objective function is non-concave in regard to variable  $\eta[l]$  and other constraints are all non-convex. Therefore, problem (P4.1) is still a non-convex problem.

Because the term  $-\log_2 \left( 1 + \frac{\hat{h}_{R,E}[l]P_R[l]}{\frac{\beta_0 P_J[l]}{\eta[l]} + \delta_a^2} \right)$  of the objective function (33a) is convex, it need to be tackled by the first order Taylor expansion and its expansion is as follow

$$-\log_2 \left( 1 + \frac{\hat{h}_{R,E}[l]P_R[l]}{\frac{\beta_0 P_J[l]}{\eta[l]} + \delta_a^2} \right) \geq -Y^{(i)}[l] - S^{(i)}[l] \left( \eta[l] - \eta^{(i)}[l] \right), l \in \mathcal{L}, \quad (34)$$

where  $Y^{(i)}[l] = \log_2 \left( 1 + \frac{\hat{h}_{R,E}[l]P_R[l]\eta^{(i)}[l]}{\beta_0 P_J[l] + \delta_a^2 \eta^{(i)}[l]} \right)$  and  $S^{(i)}[l] = \frac{\beta_0 \hat{h}_{R,E}[l]P_R[l]P_J[l]}{\ln 2 (\beta_0 P_J[l] + \delta_a^2 \eta^{(i)}[l]) (\beta_0 P_J[l] + (\delta_a^2 + \hat{h}_{R,E}[l]P_R[l])\eta^{(i)}[l])}$ . The left hand side (LHS) terms of the constraints (33e), (33f), and (33g) and the RHS term of (33h) are convex functions and they don't satisfy convex condition. Based on the first order Taylor expansion method, we can attain the lower bound of the LHS terms of (33e), (33f) and (33g) as well as the RHS term of (33h), and we have the inequalities as follows

$$\|\mathbf{q}_J[l] - \mathbf{q}_R[l]\|^2 \geq \left\| \mathbf{q}_J^{(i)}[l] - \mathbf{q}_R[l] \right\|^2 + 2 \left( \mathbf{q}_J^{(i)}[l] - \mathbf{q}_R[l] \right)^T \left( \mathbf{q}_J[l] - \mathbf{q}_J^{(i)}[l] \right), \quad (35)$$

$$\|\mathbf{q}_J[l] - \mathbf{w}_s\|^2 \geq$$

$$\left\| \mathbf{q}_J^{(i)}[l] - \mathbf{w}_s \right\|^2 + 2 \left( \mathbf{q}_J^{(i)}[l] - \mathbf{w}_s \right)^T \left( \mathbf{q}_J[l] - \mathbf{q}_J^{(i)}[l] \right), \quad (36)$$

$$\begin{aligned} & \left\| \mathbf{q}_J[l] - \mathbf{w}_{P,k} \right\|^2 \geq \\ & \left\| \mathbf{q}_J^{(i)}[l] - \mathbf{w}_{P,k} \right\|^2 + 2 \left( \mathbf{q}_J^{(i)}[l] - \mathbf{w}_{P,k} \right)^T \left( \mathbf{q}_J[l] - \mathbf{q}_J^{(i)}[l] \right). \end{aligned} \quad (37)$$

According to the inequalities (35), (36) and (37), the constraint conditions (33e), (33f), (33g) and (33h) are rewritten as

$$\left\| \mathbf{q}_J^{(i)}[l] - \mathbf{q}_R[l] \right\|^2 + 2 \left( \mathbf{q}_J^{(i)}[l] - \mathbf{q}_R[l] \right)^T \left( \mathbf{q}_J[l] - \mathbf{q}_J^{(i)}[l] \right) + \Delta H^2 \geq \mu[l], \quad (38)$$

$$\left\| \mathbf{q}_J^{(i)}[l] - \mathbf{w}_s \right\|^2 + 2 \left( \mathbf{q}_J^{(i)}[l] - \mathbf{w}_s \right)^T \left( \mathbf{q}_J[l] - \mathbf{q}_J^{(i)}[l] \right) + H_J^2 \geq \varphi[l], \quad (39)$$

$$\left\| \mathbf{q}_J^{(i)}[l] - \mathbf{q}_R[l] \right\|^2 + 2 \left( \mathbf{q}_J^{(i)}[l] - \mathbf{q}_R[l] \right)^T \left( \mathbf{q}_J[l] - \mathbf{q}_J^{(i)}[l] \right) + \Delta H^2 \geq d_{\min}^2, \quad (40)$$

$$\begin{aligned} \frac{\beta_0 P_J[l]}{\Gamma_{RJ}} & \leq \left\| \mathbf{q}_J^{(i)}[l] - \mathbf{w}_{P,k} \right\|^2 \\ & + 2 \left( \mathbf{q}_J^{(i)}[l] - \mathbf{w}_{P,k} \right)^T \left( \mathbf{q}_J[l] - \mathbf{q}_J^{(i)}[l] \right) + H_J^2. \end{aligned} \quad (41)$$

Based on above convex dispose of the objective function and the constraints, problem (P4.1) is reformulated as

$$(P4.2) : \max_{\{\mathbf{q}_J[l], \omega[l], \eta[l], \mu[r], \varphi[l]\}} \frac{1}{L} \sum_{l=1}^L \left[ \omega[l] - S^{(i)}[l] \eta[l] \right. \\ \left. - Y^{(i)}[l] + S^{(i)}[l] \eta^{(i)}[l] \right] \quad (42a)$$

$$\text{s.t. (33b), (33c), (33d), (38), (39), (40), (41), and (14g).} \quad (42b)$$

Through the convex dispose of the objective function and the constraints of (P4.1), the new problem (P4.2) is certified to be a convex optimization problem which is able to be solved by the convex optimization tool CVX. The optimal solution of (P4.2) which can satisfy the constraints of (P4.1) is the feasible solution of (P4.1). Since problem (P4.1) is equivalent to problem (P4), problem (P4.2) is also equivalent to problem (P4).

### C. Optimizing The UAV Relay's Trajectory

In this subsection, we optimize the flight trajectory  $\mathbf{q}_R[l]$  of the SUAV  $R$  with the fixed the SUAV  $J$ 's trajectory  $\mathbf{q}_J[l]$  and the transmit power  $P_J[l]$ , the SUAV  $R$ 's transmit power  $P_R[l]$  and the transmit power  $P_n[l]$  of the SIoT  $n$ . So, we are able to formulate the subproblem (P5), which is written as

$$(P5) : \max_{\{\mathbf{q}_R[l]\}} \frac{1}{L} \sum_{l=1}^L \left[ \log_2 \left( 1 + \frac{g[l]}{\|\mathbf{q}_R[l] - \mathbf{w}_s\|^2 + H_R^2} \right) \right. \\ \left. - \log_2 \left( 1 + \frac{f[l]}{(\|\mathbf{q}_R[l] - \hat{w}_e\| - \pi)^2 + H_R^2} \right) \right] \quad (43a)$$

$$\text{s.t. } \sum_{r=2}^l \log_2 \left( 1 + \frac{g[r]}{\|\mathbf{q}_R[r] - \mathbf{w}_s\|^2 + H_R^2} \right) \\ \leq \sum_{r=1}^{l-1} \sum_{n=1}^N \log_2 \left( 1 + \frac{\frac{\beta_0 P_n[r]}{\|\mathbf{q}_R[r] - \mathbf{w}_n\|^2 + H_R^2}}{\frac{\beta_0 P_J[r]}{\|\mathbf{q}_R[r] - \mathbf{q}_J[r]\|^2 + \Delta H^2} + \delta_a^2} \right), \quad (43b)$$

$$\begin{aligned} & \|\mathbf{q}_R[l+1] - \mathbf{q}_R[l]\| \leq \hat{V}_{\max}, \\ & (11), (14f) \text{ and } (14h), \end{aligned} \quad (43c) \quad (43d)$$

where  $g[l] = \frac{\beta_0 P_R[l]}{h_{J,S}[l] P_J[l] + \delta_a^2}$  and  $f[l] = \frac{\beta_0 P_R[l]}{h_{J,E}[l] P_J[l] + \delta_a^2}$ . In problem (P5), the objective function (43a) is non-concave function and the constraints (43b) and (11) are non-convex in regard to  $\mathbf{q}_R[r]$ . Therefore, problem (P5) is a non-convex problem. The slack variable  $\psi[l]$  and  $\phi[l]$  are introduced to the objective function (43a). Consider concave or linear processing for the objective function, the slack variables are expressed as  $\psi[l] = \log_2 \left( 1 + \frac{g[l]}{\|\mathbf{q}_R[l] - \mathbf{w}_s\|^2 + H_R^2} \right)$  and  $\phi[l] = (\|\mathbf{q}_R[l] - \hat{w}_e\| - \pi)^2 + H_R^2$ . We introduce slack variables  $C[r]$  and  $\rho[r]$  to define them as  $C[r] = \frac{\beta_0 P_J[r]}{\|\mathbf{q}_R[r] - \mathbf{q}_J[r]\|^2 + \Delta H^2} + \delta_a^2 + \frac{\beta_0 P_n[r]}{\|\mathbf{q}_R[r] - \mathbf{w}_n\|^2 + H_R^2}$  and  $\rho[r] = \|\mathbf{q}_R[r] - \mathbf{q}_J[r]\|^2 + \Delta H^2$ , respectively. And we have

$$\begin{aligned} & \log_2 \left( 1 + \frac{\frac{\beta_0 P_n[r]}{\|\mathbf{q}_R[r] - \mathbf{w}_n\|^2 + H_R^2}}{\frac{\beta_0 P_J[r]}{\|\mathbf{q}_R[r] - \mathbf{q}_J[r]\|^2 + \Delta H^2} + \delta_a^2} \right) \\ & = \log_2 C[r] - \log_2 \left( \frac{\beta_0 P_J[r]}{\rho[r]} + \delta_a^2 \right). \end{aligned} \quad (44)$$

By introducing multiple slack variables and new constraints, we can get new problems (P5.1), which is

$$(P5.1) : \max_{\{\mathbf{q}_R[l], \psi[l], \phi[l], C[l], \rho[l]\}} \frac{1}{L} \sum_{l=1}^L \left[ \psi[l] - \log_2 \left( 1 + \frac{f[l]}{\phi[l]} \right) \right] \quad (45a)$$

$$\text{s.t. } \sum_{r=2}^l \psi[r] \leq \sum_{r=1}^{l-1} \sum_{n=1}^N \left( \log_2 C[r] - \log_2 \left( \frac{\beta_0 P_J[r]}{\rho[r]} + \delta_a^2 \right) \right), \quad (45b)$$

$$\psi[l] \leq \log_2 \left( 1 + \frac{g[l]}{\|\mathbf{q}_R[l] - \mathbf{w}_s\|^2 + H_R^2} \right), \quad (45c)$$

$$\phi[l] \leq (\|\mathbf{q}_R[l] - \hat{w}_e\| - \pi)^2 + H_R^2, \quad (45d)$$

$$\begin{aligned} C[l] & \leq \frac{\beta_0 P_J[l]}{\|\mathbf{q}_R[l] - \mathbf{q}_J[l]\|^2 + \Delta H^2} \\ & + \delta_a^2 + \frac{\beta_0 P_n[l]}{\|\mathbf{q}_R[l] - \mathbf{w}_n\|^2 + H_R^2}, \end{aligned} \quad (45e)$$

$$\rho[l] \leq \|\mathbf{q}_R[l] - \mathbf{q}_J[l]\|^2 + \Delta H^2, \quad (45f)$$

$$(11), (14f), (14h), \text{ and } (43c). \quad (45g)$$

By adding two new constraints (45c) and (45d) in problem (P5.1), it can deduce that the transformed objective function (45a) is the lower bound of (43a) of problem (P5). The added constraints (45e) and (45f) can indicate that the RHS of (45b) is lower bound of that of (43b). In constraint (45c), the exists always a feasible solution  $\mathbf{q}_R[l]$  meet simultaneously the constraints (45b), (45c) and (43b) by reducing variable  $\psi[l]$ . Thus, the constraint (45b) is equivalent to (43b). The optimal



solution of problem (P5.1) is also the feasible solution of problem (P5). This indicates that problem (P5.1) is an approximate problem of (P5). We can observe that the objective function is a concave function, and the constraints (45b), (14f) and (43c) are convex constraint conditions. But the constraints (45c), (45d), (45e), (45f), (11) and (14h) are non-convex conditions to need to be handled. Therefore, the problem (P5.1) is still a non-convex problem.

Since the RHS of the constraints (45c), (45d), (45e), (45f), and (14h) are convex functions, which do not satisfy convex condition. The first order Taylor expansion method is applied to tackle them. Thus, we have the inequalities as follows

$$\log_2 \left( 1 + \frac{g[l]}{\|\mathbf{q}_R[l] - \mathbf{w}_s\|^2 + H_R^2} \right) \geq X^{(i)}[l] - Z^{(i)}[l] \left( \|\mathbf{q}_R[l] - \mathbf{w}_s\|^2 - \|\mathbf{q}_R^{(i)}[l] - \mathbf{w}_s\|^2 \right), \quad (46)$$

$$\|\mathbf{q}_R[l] - \hat{\mathbf{w}}_e\|^2 \geq \|\mathbf{q}_R^{(i)}[l] - \hat{\mathbf{w}}_e\|^2 + 2 \left( \mathbf{q}_R^{(i)}[l] - \hat{\mathbf{w}}_e \right)^T \left( \mathbf{q}_R[l] - \mathbf{q}_R^{(i)}[l] \right), \quad (47)$$

$$\frac{\beta_0 P_J[l]}{\|\mathbf{q}_R[l] - \mathbf{q}_J[l]\|^2 + \Delta H^2} \geq K^{(i)}[l] - M^{(i)}[l] \left( \|\mathbf{q}_R[l] - \mathbf{q}_J[l]\|^2 - \|\mathbf{q}_R^{(i)}[l] - \mathbf{q}_J[l]\|^2 \right), \quad (48)$$

$$\frac{\beta_0 P_n[l]}{\|\mathbf{q}_R[l] - \mathbf{w}_n\|^2 + H_R^2} \geq \frac{2\beta_0 P_n[l]}{\|\mathbf{q}_R^{(i)}[l] - \mathbf{w}_n\|^2 + H_R^2} - \frac{\beta_0 P_n[l] \left( H_R^2 + \|\mathbf{q}_R[l] - \mathbf{w}_n\|^2 \right)}{\left( \|\mathbf{q}_R^{(i)}[l] - \mathbf{w}_n\|^2 + H_R^2 \right)^2}, \quad (49)$$

$$\|\mathbf{q}_R[l] - \mathbf{q}_J[l]\|^2 \geq \|\mathbf{q}_R^{(i)}[l] - \mathbf{q}_J[l]\|^2 + 2 \left( \mathbf{q}_R^{(i)}[l] - \mathbf{q}_J[l] \right)^T \left( \mathbf{q}_R[l] - \mathbf{q}_R^{(i)}[l] \right), \quad (50)$$

where we define  $X^{(i)}[l] = \log_2 \left( 1 + \frac{g[l]}{\|\mathbf{q}_R^{(i)}[l] - \mathbf{w}_s\|^2 + H_R^2} \right)$ ,  $Z^{(i)}[l] = \frac{g[l]}{\ln 2 \left( \|\mathbf{q}_R^{(i)}[l] - \mathbf{w}_s\|^2 + H_R^2 \right) \left( \|\mathbf{q}_R^{(i)}[l] - \mathbf{w}_s\|^2 + H_R^2 + g[l] \right)}$ ,  $K^{(i)}[l] = \frac{\beta_0 P_J[l]}{\|\mathbf{q}_R^{(i)}[l] - \mathbf{q}_J[l]\|^2 + \Delta H^2}$  and  $M^{(i)}[l] = \frac{\beta_0 P_J[l]}{\left( \|\mathbf{q}_R^{(i)}[l] - \mathbf{q}_J[l]\|^2 + \Delta H^2 \right)^2}$ . The constraint condition (11) is

also the non-convex constraint. Due to the positive term  $\Gamma^{R,J}$  and  $\|\mathbf{q}_R[l] - \mathbf{w}_{P,k}\|^2 + H_R^2$ , we move the LHS term and the RHS term of (11) and attain new inequality as  $\frac{\beta_0 P_R[l]}{\Gamma^{R,J}} \leq \|\mathbf{q}_R[l] - \mathbf{w}_{P,k}\|^2 + H_R^2$ , the RHS term of which is tackled based on the first order Taylor expansion method as follow

$$\|\mathbf{q}_R[l] - \mathbf{w}_{P,k}\|^2 \geq \|\mathbf{q}_R^{(i)}[l] - \mathbf{w}_{P,k}\|^2$$

$$+ 2 \left( \mathbf{q}_R^{(i)}[l] - \mathbf{w}_{P,k} \right)^T \left( \mathbf{q}_R[l] - \mathbf{q}_R^{(i)}[l] \right). \quad (51)$$

According to the above convex processing for the constraint conditions of problem (P5.1), we are able to attain new optimization problem (P5.2), which is formulated as

$$(P5.2) : \max_{\left\{ \mathbf{q}_R^{[l], \psi^{[l]}, \phi^{[l], C^{[l], \rho^{[l]}} \right\}} \frac{1}{L} \sum_{l=1}^L [\psi[l] - \log_2 \left( 1 + \frac{f[l]}{\phi[l]} \right)] \quad (52a)$$

$$\text{s.t.} \sum_{r=2}^l \psi[r] \leq \sum_{r=1}^{l-1} \sum_{n=1}^N \left( \log_2 C[r] - \log_2 \left( \frac{\beta_0 P_J[r]}{\rho[r]} + \delta_a^2 \right) \right), \quad (52b)$$

$$\psi[l] \leq X^{(i)}[l] - Z^{(i)}[l] \left( \|\mathbf{q}_R[l] - \mathbf{w}_s\|^2 - \|\mathbf{q}_R^{(i)}[l] - \mathbf{w}_s\|^2 \right), \quad (52c)$$

$$\phi[l] \leq \|\mathbf{q}_R^{(i)}[l] - \hat{\mathbf{w}}_e\|^2 - 2\pi \|\mathbf{q}_R[l] - \hat{\mathbf{w}}_e\| + \pi^2 + H_R^2 + 2 \left( \mathbf{q}_R^{(i)}[l] - \hat{\mathbf{w}}_e \right)^T \left( \mathbf{q}_R[l] - \mathbf{q}_R^{(i)}[l] \right), \quad (52d)$$

$$C[l] \leq K^{(i)}[l] + \delta_a^2 + \frac{2\beta_0 P_n[l]}{\|\mathbf{q}_R^{(i)}[l] - \mathbf{w}_n\|^2 + H_R^2} - M^{(i)}[l] \left( \|\mathbf{q}_R[l] - \mathbf{q}_J[l]\|^2 - \|\mathbf{q}_R^{(i)}[l] - \mathbf{q}_J[l]\|^2 \right) - \frac{\beta_0 P_n[l] \left( H_R^2 + \|\mathbf{q}_R[l] - \mathbf{w}_n\|^2 \right)}{\left( \|\mathbf{q}_R^{(i)}[l] - \mathbf{w}_n\|^2 + H_R^2 \right)^2}, \quad (52e)$$

$$\rho[l] \leq \Upsilon^{(i)}[l] + 2 \left( \mathbf{q}_R^{(i)}[l] - \mathbf{q}_J[l] \right)^T \left( \mathbf{q}_R[l] - \mathbf{q}_R^{(i)}[l] \right), \quad (52f)$$

$$\frac{\beta_0 P_R[l]}{\Gamma^R} \leq \Psi_k^{(i)}[l] + 2 \left( \mathbf{q}_R^{(i)}[l] - \mathbf{w}_{P,k} \right)^T \left( \mathbf{q}_R[l] - \mathbf{q}_R^{(i)}[l] \right), \quad (52g)$$

$$\Upsilon^{(i)}[l] + 2 \left( \mathbf{q}_R^{(i)}[l] - \mathbf{q}_J[l] \right)^T \left( \mathbf{q}_R[l] - \mathbf{q}_R^{(i)}[l] \right) \geq d_{\min}^2, \quad (52h)$$

$$(14f) \text{ and } (43c), \quad (52i)$$

where we define  $\Upsilon^{(i)}[l] = \|\mathbf{q}_R^{(i)}[l] - \mathbf{q}_J[l]\|^2 + \Delta H^2$  and  $\Psi_k^{(i)}[l] = \|\mathbf{q}_R^{(i)}[l] - \mathbf{w}_{P,k}\|^2 + H_R^2$ . Through the dispose of constraints, the problem (P5.2) is a convex problem, which is solved by the CVX toolbox. In the problem (P5.2), the lower bound of some constraint conditions is obtained by convex processing. Thus, the attained feasible solution of problem (P5.2) meets also all constraints of problem (P5.1). This indicates that the feasible solution of problem (P5.2) is also the feasible solution of problem (P5.1). In consequence, problem (P5.2) is equivalent to problem (P5.1). Due to problem (P5.1) is equivalent to problem (P5). Therefore, the feasible solution of problem (P5.2) can satisfy all constraints of problem (P5), and problem (P5.2) is also equivalent to problem (P5.1).

Based on the alternative optimization of problems (P3.2), (P4.2) and (P5.2), the efficient algorithm is designed and summarized as Algorithm 1 to attain the optimal solution.

TABLE I  
THE ALTERNATING OPTIMIZATION ALGORITHM.

**Algorithm 1:** The alternating optimization for (P1).

1: **Initialization:**

Set the initial UAVs' trajectories as  $\{\mathbf{q}_R^{(0)}[l], \mathbf{q}_J^{(0)}[l]\}$ , and set IT thresholds  $\Gamma^{R,J}$  and  $\Gamma^S$ , the initial power values  $\{P_n^{(0)}[l], P_R^{(0)}[l], P_J^{(0)}[l]\}$ , the rang estimation value  $\pi$  as well as the accuracy  $\theta$ .

2: **Repeat :**

3: Under the given UAVs' trajectories  $\mathbf{q}_R^{(i)}[l]$  and  $\mathbf{q}_J^{(i)}[l]$ , and the calculated  $A^{(i)}[l]$  and  $B^{(i)}[l]$ , obtain the optimal power allocation  $\{P_n^{(i+1)}[l], P_R^{(i+1)}[l], P_J^{(i+1)}[l]\}$  by solving (P3.2).

4: With the given  $\{P_n^{(i+1)}[l], P_R^{(i+1)}[l], P_J^{(i+1)}[l]\}$  and  $\mathbf{q}_R^{(i)}[l]$ , and the calculated  $\eta^{(i)}[l]$ , acquire the optimized trajectory  $\mathbf{q}_J^{(i+1)}[l]$  of the UAV  $J$  by solving (P4.2).

5: For the given  $\{P_n^{(i+1)}[l], P_R^{(i+1)}[l], P_J^{(i+1)}[l]\}$  and  $\mathbf{q}_J^{(i+1)}[l]$ , attain the optimized trajectory  $\mathbf{q}_R^{(i+1)}[l]$  of the UAV  $R$  by solving (P5.2).

6: Update the iterative number  $i = i + 1$ .

7: **Until** the objective value of (P5.2) converges within a given accuracy  $\theta$ .

8: **Obtain solutions:**

$P_n^{opt}[l], P_R^{opt}[l], P_J^{opt}[l], \mathbf{q}_J^{opt}[l]$  and  $\mathbf{q}_R^{opt}[l]$ .

Since the problems (P3.2), (P4.2) and (P5.2) are sub problems of the original problem (P1). Hence, the optimal solutions of (P3.2), (P4.2) and (P5.2) are the sub optimal solution of (P1). According to the algorithm complexity analysis of the literatures [43], [44], the total algorithm complexity is composed of the iteration number of SCA method, iteration complexity and the per-iteration computation cost. In Algorithm 1, the iteration number of SCA method is  $F$ . The iteration complexity and the per iteration computation cost are computed as  $O(\sqrt{NL} \cdot \ln(\theta^{-1}))$  and  $O(NL)$ , respectively. Therefore, we can calculate the total complexity of the proposed Algorithm 1 which is written as  $O(F \ln(\theta^{-1}) N^{\frac{3}{2}} L^{\frac{3}{2}})$ .

#### IV. SIMULATION RESULTS

In this section, numerical results are offered to evaluate the performance of the proposed Algorithm 1. In the cognitive system, we set the initial horizontal positions of the UAV  $R$  and the UAV  $J$  as  $\mathbf{q}_R^{ini} = (0, 400 \text{ m})$  and  $\mathbf{q}_J^{ini} = (0, -1000 \text{ m})$ , and their final locations in horizontal direction as  $\mathbf{q}_R^{fin} = (3500 \text{ m}, 400 \text{ m})$  and  $\mathbf{q}_J^{fin} = (3500 \text{ m}, -1000 \text{ m})$ , respectively. During the UAVs' flight from the initial site to the final site, they all keep the fixed altitude  $H_R = H_J = 30 \text{ m}$  to fly within the maximum limit speed  $V_{\max} = 30 \text{ m/s}$ . In order to avoid collision for the UAV  $R$  and the UAV  $J$  each other, the minimum safety distance is set as  $d_{\min} = 10 \text{ m}$ . Suppose that there are three SIoT, i.e.,  $N = 3$  and a SU in the secondary network, and they are marked with blue asterisks and blue hexagon in the simulation diagram, respectively. For the average transmit powers of the SIoT, the UAV  $R$  and the UAV  $J$ , we set them as  $\bar{P}_T = 20 \text{ dBm}$ ,  $\bar{P}_R = 20 \text{ dBm}$

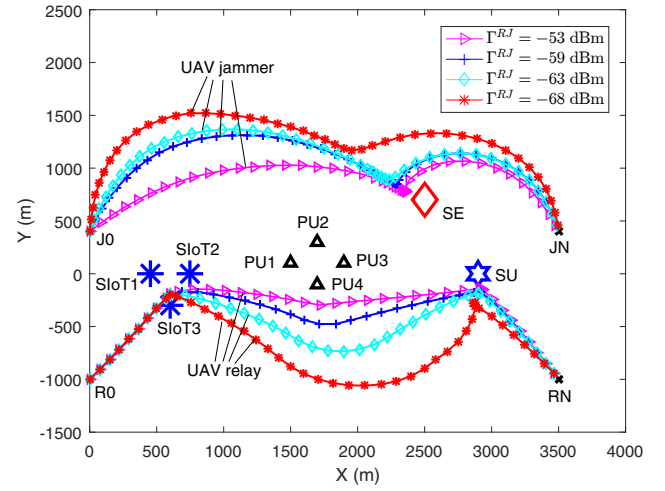


Fig. 2. The optimized trajectories of the SUAVs based on different IT thresholds.

and  $\bar{P}_J = 20 \text{ dBm}$ , respectively. Meanwhile, the maximum transmit powers of the SIoT, the SUAV  $R$  and the SUAV  $J$  are set as  $P_T^{\max} = 26 \text{ dBm}$ ,  $P_R^{\max} = 26 \text{ dBm}$ , and  $P_J^{\max} = 26 \text{ dBm}$ , respectively. In the primary network, it is supposed that there are four the PUs, i.e.,  $K = 4$  PUs, and a SE, which are marked by using four black triangles and a red rhombus in the diagram, respectively. The reference power gain of channel is set as  $\beta_0 = -30 \text{ dB}$  and the total interference power  $\delta_a^2$  is set as  $\delta_a^2 = -80 \text{ dBm}$  [24]. For the constraint (10), the path loss exponent is set as  $\lambda = 3$  [45]. Since the interference threshold  $\Gamma^S$  caused by the transmit power of the SIoT  $n$  for the PUs has no big influence on the trajectories optimization of the SUAVs and the secrecy rate of the secondary relay network, the  $\Gamma^S$  is set as the fixed value, i.e.,  $\Gamma^S = -91 \text{ dBm}$ .

Fig. 2 shows the optimized trajectories of the SUAV  $R$  and the UAV  $J$  based on the different IT threshold  $\Gamma^{R,J}$  with the total flight time 180 s and the maximum range estimation value  $\pi = 20$ . In Fig. 2, the SUAV  $R$  first flies to the sky above the SIoT from the initial point in order to receive rapidly information with the good links. When the SUAV  $R$  flies through the area of the PUs in Fig. 2, we can observe that the SUAV  $R$  keeps away from the PUs. That is because that the distance interval between the SUAV  $R$  and the PUs can protect the PUs of the primary network from the interference generated by the SUAV  $R$ . From the observation of Fig. 2, the SUAV  $R$  flies close to the SU in order to transmit more information to the SU within the limited flight time. In Fig. 2, we can observe that the optimized trajectories of the SUAV  $R$  and the SUAV  $J$  are different with the different IT thresholds  $\Gamma^{R,J}$ . When we set the tolerant IT threshold as  $\Gamma^{R,J} = -53 \text{ dBm}$ , the optimized trajectories of the SUAV  $R$  and the SUAV  $J$  are closest to the PUs. When the  $\Gamma^{R,J}$  is set as  $\Gamma^{R,J} = -68 \text{ dBm}$ , the SUAV  $R$  and the SUAV  $J$  are farthest to the PUs. This indicates that the PUs are more sensitive to the interferences from the SUAV  $R$  and the SUAV  $J$  when IT threshold value  $\Gamma^{R,J}$  is more smaller. About the optimized trajectory of the SUAV  $J$  in Fig. 2, it is observed

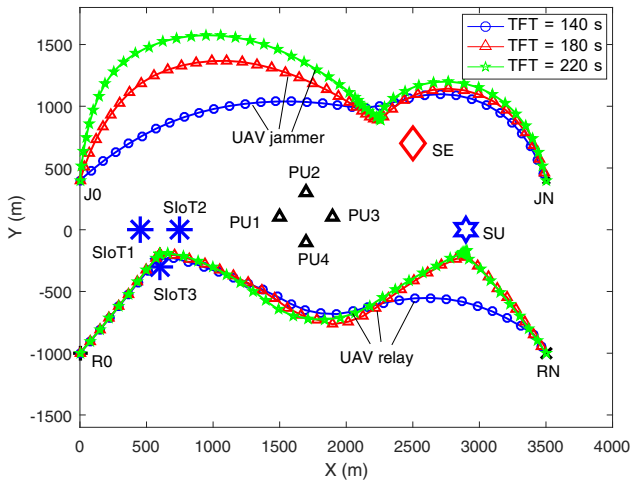


Fig. 3. The SUAVs' optimization trajectories under different flight time.

that the SUAV  $J$  not only keeps away from the PUs, but also is far away from the SUAV  $R$  in the most time slots. That is because that the transmit power of the friendly SUAV  $J$  also cause interference for the SUAV  $R$  and the PUs. As shown in Fig. 2, when the SUAV  $J$  flies through the SE, the SUAV  $J$  will try to get close to the SE. That is because that the SUAV  $J$  can transmit a mass of the disturbed information to the SE in order to improve the secrecy rate of the secondary relay network.

Fig. 3 shows the optimized trajectories of the SUAV  $R$  and the SUAV  $J$  based on the different total flight time under the tolerant IT threshold  $\Gamma^{R,J} = -63$  dBm and  $\pi = 20$ . By viewing the SUAV  $R$ 's optimization trajectory in Fig. 3, the SUAV  $R$  cannot fly close enough to the SU when the total flight time is set as 140 s, i.e.,  $TFT = 140$  s. That is because that the SUAV  $R$  does not have enough time to do more missions when the limited flight time is set as  $TFT = 140$  s. When the total flight time is set as  $TFT = 220$  s, we can observe from Fig. 3 that when the SUAV  $R$  hovers over the SloTs and the SU for some time slots, especially over the SU. This indicates that the SUAV  $R$  can collect and transmit more information in the secondary network as the total flight time is sufficient. For the comparison of the SUAV  $J$ 's optimization trajectory with three different flight time in Fig. 3, it is observed that the SUAV  $J$  is given more time, the SUAV  $J$  is more far away from the PUs and the SUAV  $R$  in order to decrease the interference for them. At the same time, we also observe that the SUAV  $J$  hovers over the SE for longer time under the sufficient flight time so as to be able to enhance the secrecy rate of the secondary network.

Fig. 4 shows the change of the optimized power for the SloTs, the SUAV  $R$  and the SUAV  $J$  with the change of time  $T$  based on the IT threshold  $\Gamma^{R,J} = -63$  dBm, the total flight time 180 s and  $\pi = 20$ . In Fig. 4, it is observed that the power values of three SloTs first increase rapidly to their peak value, and then decline slowly to zero value. That is because that the SUAV  $R$  flies close to the SloTs and collects rapidly more information by increasing the transmit power of the SloTs. When the SUAV  $R$  flies away the SloTs, the SloTs decline

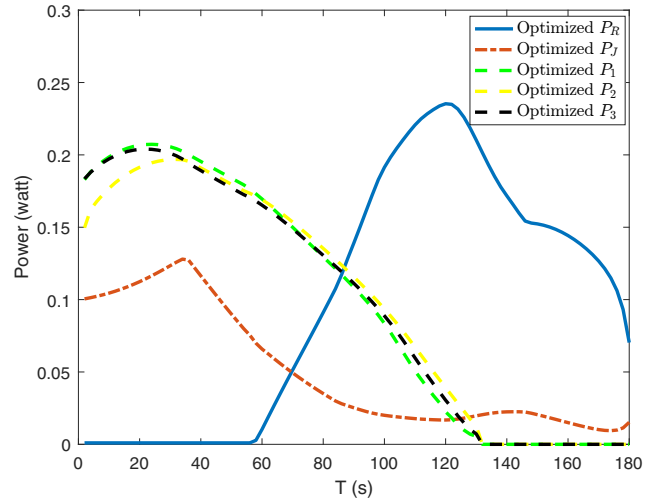


Fig. 4. Change of optimization power versus time  $T$ .

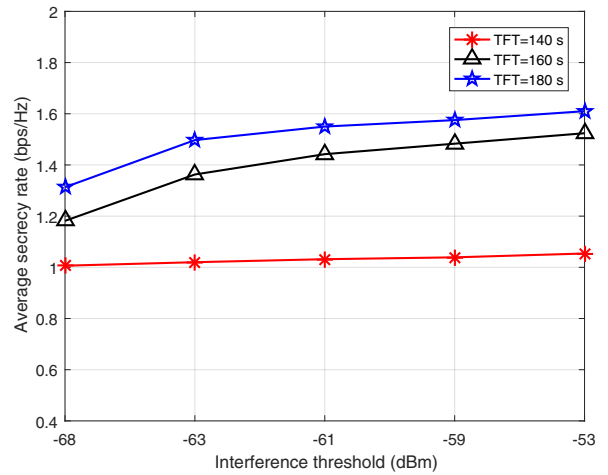


Fig. 5. The average secrecy rates of the secondary relay network based on different IT thresholds and different total flight time.

their transmit power due to the power constraint and the IT threshold constraint. From Fig. 4, we can observe that the power value of the SUAV  $R$  increases slowly from zero to a maximum value and then decreases slowly to a certain value. However, the change curve of the power value for the SUAV  $J$  has an opposite trend in comparison with the change curve of the power for the SUAV  $R$  in Fig. 4. That indicates that the SUAV  $R$  only collects information and does not delivery information in the beginning period, in which the SUAV  $J$  transmits a mass of interference data to the SE by increasing transmit power under the IT threshold constraint. When the SUAV  $R$  delivery information to the SU by gradually enlarging the transmit power, the SUAV  $J$  will reduce its transmit power yet in order to decrease the interference for the SUAV  $R$ 's communication.

Fig. 5 shows the the change of average secrecy rates of the secondary relay network based on different IT thresholds  $\Gamma^{R,J}$  and different total flight time under  $\pi = 20$ . We can observe from Fig. 5 that the average secrecy rate of the secondary

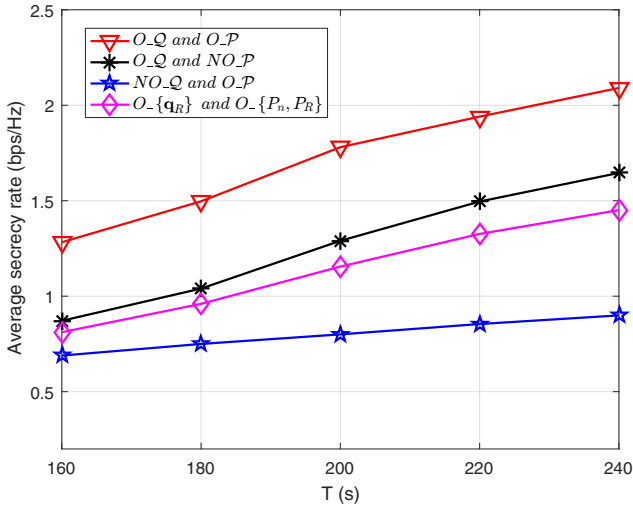


Fig. 6. The average secrecy rates of the secondary relay network versus the total flight time  $T$  based on the different optimization schemes.

relay network increases with the increase of the interference threshold value at same total flight time. We can also observe that the average secrecy rate of the secondary relay network increases as the total flight time increases under same the interference threshold value. By combining Figs. 2 and 3 to analyze the simulation result of Fig. 5, we can obtain that the SUAV  $R$  can collect and transmit more information to the SU by flying closer to the SIoTs and the SU to improve the average secrecy rate of the secondary relay network when the IT threshold  $\Gamma^{RJ}$  and the total flight time are set to a relatively large value. Likewise, the SUAV  $J$  can fly close to the SE and transmit more disturbed information to the SE under the larger IT threshold  $\Gamma^{RJ}$  value and more flight time so as to improve the average secrecy rate of the secondary relay network.

Fig. 6 shows the change of the average secrecy rates of the secondary relay network versus the total flight time  $T$  based on four optimization schemes under  $\Gamma^{RJ} = -63$  dBm and  $\pi = 20$ . It is clearly observed that the average secrecy rates of the four optimization schemes all go up as the total flight time of the SUAVs increases. In Fig. 6, the symbols  $O_Q$  and  $NO_Q$  denote the optimization trajectories of the SUAVs and no optimization trajectories of the SUAVs, respectively. Likewise, the symbols  $O_P$  and  $NO_P$  represent the optimization power of the SUAVs and no optimization power of the SUAVs, respectively. The first optimization scheme is denoted by  $O_Q$  and  $O_P$  in Fig. 6. The first optimization scheme which is our proposed optimization scheme of jointly optimizing the SUAVs' trajectories and power is an optimum optimization scheme by comparing with other three optimization schemes. Via the comparison of the first optimization scheme and the fourth optimization scheme which is no SUAV  $J$  scheme denoted by  $O_{\{q_R\}}$  and  $O_{\{P_n, P_R\}}$  in Fig. 6, the average secrecy rate of the former is higher than that of the latter. This indicates that the SUAV  $J$  which is friendly added by disturbing the SE can help the secondary relay network to better improve the average secrecy rate of the system. By comparing the second optimization scheme denoted by  $O_Q$

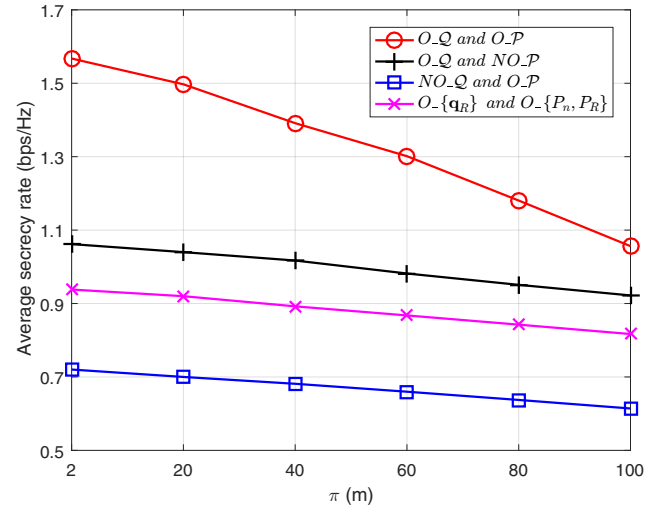


Fig. 7. The average secrecy rates of the secondary relay network versus the range estimation value  $\pi$  based on the different optimization schemes.

and  $NO_P$  with the third optimization scheme denoted by  $NO_Q$  and  $O_P$  in Fig. 6, we can obtain the conclusion that the trajectory optimization strategy can better improve the average secrecy rate of the system than the power optimization strategy.

Fig. 7 shows the change of the average secrecy rates of the secondary relay network versus the range estimation value  $\pi$  based on four optimization schemes under  $\Gamma^{RJ} = -63$  dBm and the total flight time 180 s. In Fig. 7, we can clearly observe that the average secrecy rates of the four optimization schemes all fall off as the range estimation value  $\pi$  increases. This is because that the range estimation value  $\pi$  is set as bigger value so as to make it harder to estimate the exact location of the SE and lead to the decline of the average secrecy rates. In Fig. 7, the first optimization scheme denoted by  $O_Q$  and  $O_P$  is the best scheme which is our proposed scheme in four schemes. Via the comparison of the first optimization scheme and the fourth optimization scheme which is no SUAV  $J$  scheme denoted by  $O_{\{q_R\}}$  and  $O_{\{P_n, P_R\}}$  in Fig. 7, it is proved again that the SUAV  $J$  can help to improve the average secrecy rate of the cognitive secondary system. By comparing the second optimization scheme denoted by  $O_Q$  and  $NO_P$  with the third optimization scheme denoted by  $NO_Q$  and  $O_P$  in Fig. 7, it is also proved again that the trajectory optimization strategy can better improve the average secrecy rate of the system than the power optimization strategy. Via the comparison of the first optimization scheme and the second optimization scheme, this shows that the increased power optimization can improve the secrecy rate than no power optimization under same trajectory optimization strategies. For the comparison of the first optimization scheme and the third optimization scheme, we can observe the advantage of trajectory optimization strategy in improvement of the secrecy rate. It can be observed that the increased trajectory optimization of the SUAV  $J$  can slightly improve the secrecy rate than the increased power optimization of the SUAV  $R$  and SIoT  $n$  by comparing the second optimization scheme with the

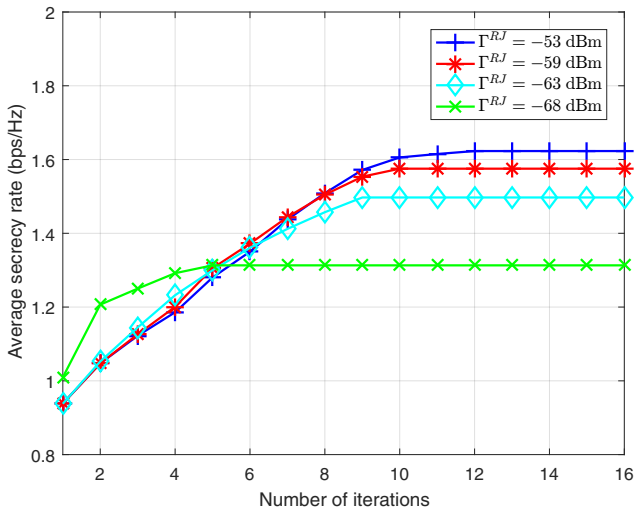


Fig. 8. Convergence of Algorithm 1 with different tolerant IT thresholds.

fourth optimization scheme. For the third optimization scheme based on no optimization trajectories of the SUAV  $R$  and the SUAV  $J$ , it is the worse scheme than the fourth optimization scheme. This also reflects the importance and advantage of trajectory optimization in improvement of the secrecy rate.

Fig. 8 shows convergence of Algorithm 1 based on four tolerant IT thresholds under the total time 180 s and  $\pi = 20$ . As shown in Fig. 8, we can observe that four curves can quickly rise to a convergence value. It indicates that Algorithm 1 can rapidly converge. For instance, the average secrecy rate based on the IT threshold  $\Gamma^{R,J} = -68$  dBm and  $\Gamma^{R,J} = -53$  dBm converge to a constant value by five iterations and eleven iterations, respectively. From Fig. 8, it is also observed that the smaller the tolerant IT threshold is set, the faster Algorithm 1 converges. The fast convergence of Algorithm 1 also proves the effectiveness of our proposed algorithm.

## V. CONCLUSION

In this paper, we studied a physical layer security issue in SUAVs-assisted cognitive relay system, where the SUAV  $R$  delivered information from the SIoTs to the SU under the spectrum sharing with the PUs. A friendly SUAV  $J$  is employed to confuse the SE to improve the security performance of the cognitive secondary system. In order to maximize the average worst-case secrecy rate, we jointly optimized robust trajectories and power of the SUAV  $R$  and the SUAV  $J$ , subject to the power, trajectories, information causality and IT threshold constraints. The original optimization problem which was a non-convex problem was divided into three sub-problems to attain locally optimal solution by using the SCA technology and the alternating optimization method. Simulations demonstrated that our proposed algorithm can effectively improve the average worst-case secrecy rate of the secondary UAV relay network in comparison with other benchmark schemes.

## REFERENCES

- [1] F. Nait-Abdesselam, A. Alsharoa, M. Y. Selim, D. Qiao, and A. E. Kamal, "Towards enabling unmanned aerial vehicles as a service for heterogeneous applications," *J. Commun. Netw.*, vol. 23, no. 3, pp. 212–221, Jun. 2021.
- [2] J. Pokorny *et al.*, "Concept design and performance evaluation of UAV-based backhaul link with antenna steering," *J. Commun. Networks*, vol. 20, no. 5, pp. 473–483, Oct. 2018.
- [3] Z. Wang, G. Zhang, Q. Wang, K. Wang, and K. Yang, "Completion time minimization in wireless-powered UAV-assisted data collection system," *IEEE Commun. Lett.*, vol. 25, no. 6, pp. 1954–1958, Jun. 2021.
- [4] H. Zhang, L. Song, Z. Han, and H. V. Poor, "Cooperation techniques for a cellular internet of unmanned aerial vehicles," *IEEE Wireless Commun. Lett.*, vol. 26, no. 5, pp. 167–173, Oct. 2019.
- [5] Z. Wang, W. Xu, D. Yang, and J. Lin, "Joint trajectory optimization and user scheduling for rotary-wing UAV-enabled wireless powered communication networks," *IEEE Access*, vol. 7, pp. 181369–181380, 2019.
- [6] Z. Wang, M. Wen, S. Dang, L. Yu, and Y. Wang, "Trajectory design and resource allocation for UAV energy minimization in a rotary-wing UAV-enabled WPCN," *Alexandria Eng. J.*, vol. 60, no. 1, pp. 1787–1796, Feb. 2021.
- [7] Liu, S.-J. Yoo, and K. S. Kwak, "Opportunistic relaying for low-altitude UAV swarm secure communications with multiple eavesdroppers," *J. Commun. Networks*, vol. 20, no. 5, pp. 496–508, Oct. 2018.
- [8] Zhang, Y. Xu, J. Loo, D. Yang, and L. Xiao, "Joint computation and communication design for UAV-assisted mobile edge computing in IoT," *IEEE Trans. Ind. Inf.*, vol. 16, no. 8, pp. 5505–5516, Aug. 2020.
- [9] H. Sun, F. Zhou, and R. Q. Hu, "Joint offloading and computation energy efficiency maximization in a mobile edge computing system," *IEEE Trans. Veh. Technol.*, vol. 68, no. 3, pp. 3052–3056, Mar. 2019.
- [10] Y. Chen *et al.*, "Optimum placement of UAV as relays," *IEEE Commun. Lett.*, vol. 22, no. 2, pp. 248–251, 2018.
- [11] F. Rongfei *et al.*, "Optimal node placement and resource allocation for UAV relaying network," *IEEE Commun. Lett.*, vol. 22, no. 4, pp. 808–811, 2018.
- [12] Y. Chen *et al.*, "Multiple UAVs as relays: Multi-hop single link versus multiple dual-hop links," *IEEE Trans. Wireless Commun.*, vol. 17, no. 9, pp. 6348–6359, 2018.
- [13] L. Li *et al.*, "UAV positioning and power control for two-way wireless relaying," *IEEE Trans. Wireless Commun.*, vol. 19, no. 2, pp. 1008–1024, 2020.
- [14] Y. Zeng, R. Zhang, and T. J. Lim, "Throughput maximization for UAV-enabled mobile relaying systems," *IEEE Trans. Commun.*, vol. 64, no. 12, pp. 4983–4996, Dec. 2016.
- [15] Sun, D. Yang, L. Xiao, L. Cuthbert, F. Wu and Y. Zhu, "Joint energy and trajectory optimization for UAV-enabled relaying network with multi-pair users," *IEEE Trans. Cognit. Commun. Netw.*, vol. 7, no. 3, pp. 939–954, Sep. 2021.
- [16] X. Zhong, Y. Guo, N. Li and Y. Chen, "Joint optimization of relay deployment, channel allocation, and relay assignment for UAVs-aided D2D networks," *IEEE/ACM Trans. Netw.*, vol. 28, no. 2, pp. 804–817, Apr. 2020.
- [17] S. Zhang *et al.*, "Joint trajectory and power optimization for UAV relay networks," *IEEE Commun. Lett.*, vol. 22, no. 1, pp. 161–164, 2018.
- [18] S. Zeng, H. Zhang, and L. Song, "Trajectory optimization and resource allocation for multi-user OFDMA UAV relay networks," in *Proc. IEEE GLOBECOM*, 2019.
- [19] X. Liang *et al.*, "Throughput optimization for cognitive UAV networks: a three-dimensional-location-aware approach," *IEEE Wireless Commun. Lett.*, vol. 9, no. 7, pp. 948–952, Jul. 2020.
- [20] Z. Wang, F. Zhou, Y. Wang, and Q. Wu, "Joint 3D trajectory and resource optimization for a UAV relay-assisted cognitive radio network," *China Commun.*, vol. 18, no. 6, pp. 184–200, Jun. 2021.
- [21] Y. Zhou, F. Zhou, H. Zhou, D. W. K. Ng, and R. Q. Hu, "Robust trajectory and transmit power optimization for secure UAV-enabled cognitive radio networks," *IEEE Trans. Commun.*, vol. 68, no. 7, pp. 4022–4034, Jul. 2020.
- [22] N. Tang, H. Tang, B. Li, and X. Yuan, "Cognitive NOMA for UAV-enabled secure communications: joint 3D trajectory design and power allocation," *IEEE Access*, vol. 8, pp. 159965–159978, 2020.
- [23] P. X. Nguyen, H. V. Nguyen, V. Nguyen, and O. Shin, "UAV-enabled jamming noise for achieving secure communications in cognitive radio networks," in *Proc. IEEE CCNC*, 2019.



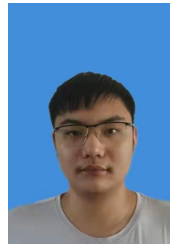
- [24] Y. Huang *et al.*, "Cognitive UAV communication via joint maneuver and power control," *IEEE Trans. Commun.*, vol. 67, no. 11, pp. 7872–7888, 2019.
- [25] Y. Chen, Z. Zhang, and B. Li, "Secure transmission with a cooperative UAV-enabled jammer," in *Proc. IEEE ICC*, 2019.
- [26] B. Duo, J. Luo, Y. Li, H. Hu, and Z. Wang, "Joint trajectory and power optimization for securing UAV communications against active eavesdropping," *China Commun.*, vol. 18, no. 1, pp. 88–99, Jan. 2021.
- [27] H. Zhang, X. He, and H. Dai, "Secure UAV communication networks via friendly jamming and bandwidth allocation," in *Proc. IEEE INFOCOM*, 2020.
- [28] A. Li and W. Zhang, "Mobile jammer-aided secure UAV communications via trajectory design and power control," *China Commun.*, vol. 15, no. 8, pp. 141–151, Aug. 2018.
- [29] R. Ma, W. Yang, Y. Zhang, J. Liu, and H. Shi, "Secure mmwave communication using UAV-enabled relay and cooperative jammer," *IEEE Access*, vol. 7, pp. 119729–119741, 2019.
- [30] R. Li *et al.*, "Resource allocation for secure multi-UAV communication systems with multi-eavesdropper," *IEEE Trans. Commun.*, vol. 68, no. 7, pp. 4490–4506, Jul. 2020.
- [31] Y. Gao, H. Tang, B. Li, and X. Yuan, "Securing energy-constrained UAV communications against both internal and external eavesdropping," *IEEE Commun. Lett.*, vol. 25, no. 3, pp. 749–753, Mar. 2021.
- [32] M. Kim, S. Kim, and J. Lee, "Securing communications with friendly unmanned aerial vehicle jammers," *IEEE Trans. Veh. Technol.*, vol. 70, no. 2, pp. 1972–1977, Feb. 2021.
- [33] B. Zhong, J. Yao, and J. Xu, "Secure UAV communication with cooperative jamming and trajectory control," *IEEE Commun. Lett.*, vol. 23, no. 2, pp. 286–289, Feb. 2019.
- [34] U. Mengali and A. N. D. Andrea, *Synchronization Techniques for Digital Receivers*. New York, NY, USA: Springer, 1997.
- [35] G. Xie, B. Wang, F. Gao, and S. Jin, "Full-space spectrum-sharing strategy for TDD/FDD massive MIMO cognitive radio systems," in *Proc. IEEE ICCS*, 2016.
- [36] S. Cherian and S. N. Shiras, "Spectrum sensing of SC-FDMA signals in cognitive radio networks," in *Proc. IEEE NetACT*, 2017.
- [37] Q. Wang, H.-N. Dai, H. Wang, G. Xu, and A. K. Sangaiah, "UAV-enabled friendly jamming scheme to secure industrial Internet of things," *J. Commun. Networks*, vol. 21, no. 5, pp. 481–490, Oct. 2019.
- [38] H. Zhou *et al.*, "Robust an-aided beamforming and power splitting design for secure miso cognitive radio with swipt," *IEEE Trans. Wireless Commun.*, vol. 16, no. 4, pp. 2450–2464, 2017.
- [39] R. Zhang *et al.*, "Dynamic resource allocation in cognitive radio networks," *IEEE Signal Process. Mag.*, vol. 27, no. 3, pp. 102–114, 2010.
- [40] A. Li *et al.*, "UAV-enabled cooperative jamming for improving secrecy of ground wiretap channel," *IEEE Wireless Commun. Lett.*, vol. 8, no. 1, pp. 181–184, 2019.
- [41] Y. Gao, H. Tang, B. Li, and X. Yuan, "Robust trajectory and power control for cognitive UAV secrecy communication," *IEEE Access*, vol. 8, pp. 49338–49352, 2020.
- [42] S. Boyd and L. Vandenberghe, *Convex optimization.*, Cambridge, U.K.: Cambridge Univ. Press, 2004.
- [43] K.-Y. Wang *et al.*, "Outage constrained robust transmit optimization for multiuser miso downlinks: Tractable approximations by conic optimization," *IEEE Trans. Signal Process.*, vol. 62, no. 21, pp. 5690–5705, 2014.
- [44] Z. Nesterov and A. Nemirovskii, *Interior-point polynomial algorithms in convex programming.* SIAM, 1994.
- [45] G. Zhang *et al.*, "Securing uav communications via joint trajectory and power control," *IEEE Trans. Wireless Commun.*, vol. 18, no. 2, pp. 1376–1389, 2019.



**Zhen Wang** received the B.S. degree from the School of Information Engineering, Nanchang University, Nanchang, China, in 2007. He is currently working toward his Ph.D. degrees at the School of Artificial Intelligence in Beijing University of Posts and Telecommunications (BUPT). He is also an Associate Professor with the School of Information Engineering, Nanchang University. His research interests include convex optimization, energy harvesting, UAV communications and networks, and wireless resource allocation.



**Jichang Guo** is a Master Candidate in School of Information Engineering at Nanchang University. He received the B.S. degree from Huangshan University, Huangshan, China, in 2020. His research interests include convex optimization, UAV communications.



**Zhiqiong Chen** is a Master Candidate in School of Information Engineering at Nanchang University. He received the B.S. degree from Nanchang Hangkong University, Nanchang, China, in 2020. His research interests include convex optimization, UAV communications.



**Lisu Yu** received the Ph.D. degree at Key Laboratory of Information Coding and Transmission, Southwest Jiaotong University, Chengdu, China. He was a Visiting Scholar at University of Arkansas, Fayetteville, AR, USA and University of Houston, Houston, TX, USA from 2017 to 2019. He has served as the Student Activities Chair of IEEE Communication Society Chengdu Chapter and several international conferences technical program committee (TPC) member, Section Chair and Special Track Chair. He is now serving as an Area Editor of the Elsevier Physical Communication, Editors of the Elsevier Computer Communications, PeerJ Computer Science, PLOS ONE, and Frontiers in Signal Processing for Communications, a Managing Guest Editor of Elsevier Internet of Things and Cyber-Physical Systems, and an Associate Area Editor of Journal of Electronics Information Technology and IEEE Communications Society Technical Committee on Green Communications and Computing (TCGCC) and Signal Processing and Computing for Communications (SPCC) Members. He is currently an Associate Professor in School of Information Engineering, Nanchang University, China. His main research interests include advanced wireless communications, coded modulation, non-orthogonal multiple access (NOMA), fiber wireless communication, ultra-dense network (UDN), unmanned aerial vehicle (UAV), and visible light communication (VLC).



**Yuhao Wang** received the Ph.D. degree from Wuhan University, Wuhan, China, in 2006. He was a Visiting Professor at Department of Electrical Communication Engineering, University of Calgary, Calgary, AB, Canada, in 2008, and also with China National Mobile Communication Research Laboratory, Southeast University, Nanjing, China, from 2010 to 2011. He is currently a Professor with the Cognition Sensor Network Laboratory, School of Information Engineering, Nanchang University (NCU), Nanchang, China. He is the Vice President of Shangrao Normal University, and also is the Deans of the Artificial Intelligence Industry Institute, NCU. Since 2016, he is an IET Fellow. His current research interests include wideband wireless communication and radar sensing fusion system, channel measurement and modeling, nonlinear signal processing, smart sensor, image and video processing, and machine learning.



**Hong Rao** is currently a Professor with the Computer Center, Nanchang University. She has published more than 30 papers in academic journals and international conferences. Her major research interests include machine learning, data mining, and intelligent information processing. She hosts several national science and technology projects and Jiangxi technology projects.